

REPORT No. 677

WIND-TUNNEL INVESTIGATION OF AN N. A. C. A. 23021 AIRFOIL WITH VARIOUS ARRANGEMENTS OF SLOTTED FLAPS

By CARL J. WENZINGER and THOMAS A. HARRIS

SUMMARY

An investigation has been made in the N. A. C. A. 7- by 10-foot wind tunnel of a large-chord N. A. C. A. 23021 airfoil with several arrangements of 25.66-percent-chord slotted flaps to determine the section aerodynamic characteristics as affected by slot shape, flap shape, flap location, and flap deflection. The flap positions for maximum lift, the polars for arrangements considered favorable for take-off and climb, and the complete section aerodynamic characteristics for selected optimum arrangements were determined. A discussion is given of the relative merits of the various arrangements for certain selected criterions. A comparison is made of a slotted flap on the N. A. C. A. 23021 airfoil with a corresponding slotted flap previously developed for the N. A. C. A. 23012 airfoil.

The best slotted-flap arrangement on the N. A. C. A. 23021 airfoil gave the same maximum lift coefficient as the best slotted flap on the N. A. C. A. 23012 airfoil. The drag coefficients were higher with the N. A. C. A. 23021 airfoil, but the pitching-moment coefficients were about equal for comparable arrangements.

INTRODUCTION

The National Advisory Committee for Aeronautics is undertaking an extensive investigation of various wing-flap combinations to furnish information applicable to the aerodynamic design of high-lift devices for improving the safety and the performance of airplanes. A high-lift device capable of producing high lift with variable drag for landing and high lift with low drag for take-off and initial climb is believed to be desirable. Other desirable aerodynamic features are: no increase in drag with the flap neutral; small change in pitching moment with flap deflection; low forces required to operate the flap; and freedom from possible hazard due to icing.

A very promising arrangement of a simple slotted flap developed for the N. A. C. A. 23012 airfoil is reported in reference 1. Further improvement, from a consideration of high lift coefficients and low drag at high and intermediate lift coefficients, was obtained by the addi-

tion of an auxiliary slotted flap to the main flap (reference 2). Another type of slotted flap, aerodynamically superior but structurally more complicated, is the venetian-blind flap reported in reference 3. All these flap arrangements were tested on the N. A. C. A. 23012 airfoil.

In the present report, the results are given of the tests of a relatively thick airfoil, the N. A. C. A. 23021, with several arrangements of 25.66-percent-chord slotted flaps. This investigation included two flap shapes, each of which was tested with several slot shapes.

MODELS

PLAIN AIRFOIL

The basic wing, or the plain airfoil, used in these tests was built to the N. A. C. A. 23021 profile and has a chord of 3 feet and a span of 7 feet; the ordinates for the section are given in table I. The model was built with solid laminated mahogany nose and trailing-edge pieces and solid mahogany ribs. The portion between the nose and the trailing edge was covered with tempered wallboard. The trailing-edge section of this model was easily removable so that the model could be quickly altered for tests of different flap arrangements.

SLOTTED FLAPS

The slotted flaps and the slot shapes were built of solid laminated mahogany. The slot shapes were bolted to the main airfoil in place of the solid trailing edge. The flaps were mounted on special hinges that permitted considerable latitude in the location of the flaps with respect to the main airfoil.

Flaps.—Two flap shapes were tested. Flap 1 (fig. 1 and table I), corresponding to flap 1 of reference 1, has a small nose radius and was designed to give only a small break in the airfoil lower surface when undeflected. It also lends itself to use with a door to seal the break in the lower surface of the airfoil with the flap undeflected.

Flap 2 corresponds to flap 2 of reference 1, which gave the lowest drag at high and intermediate lift coefficients on the N. A. C. A. 23012 airfoil. This flap is shown in figure 2 and its ordinates are given in table I. This flap shape was obtained by combining the nose of

an N. A. C. A. 6330 airfoil with the trailing-edge portion of the main wing. It was designed to give low drag at intermediate and high lift coefficients.

Slot shapes.—Slot shape a, which was used in combination with both flaps, is shown in figures 1 (a) and 2 (a). This slot shape was designed to give a minimum break in the lower surface of the wing and, consequently, to have the smallest effect on the drag with the flap neutral. Slot shape b is similar to slot shape h of reference 1, which gave the lowest drag at intermediate

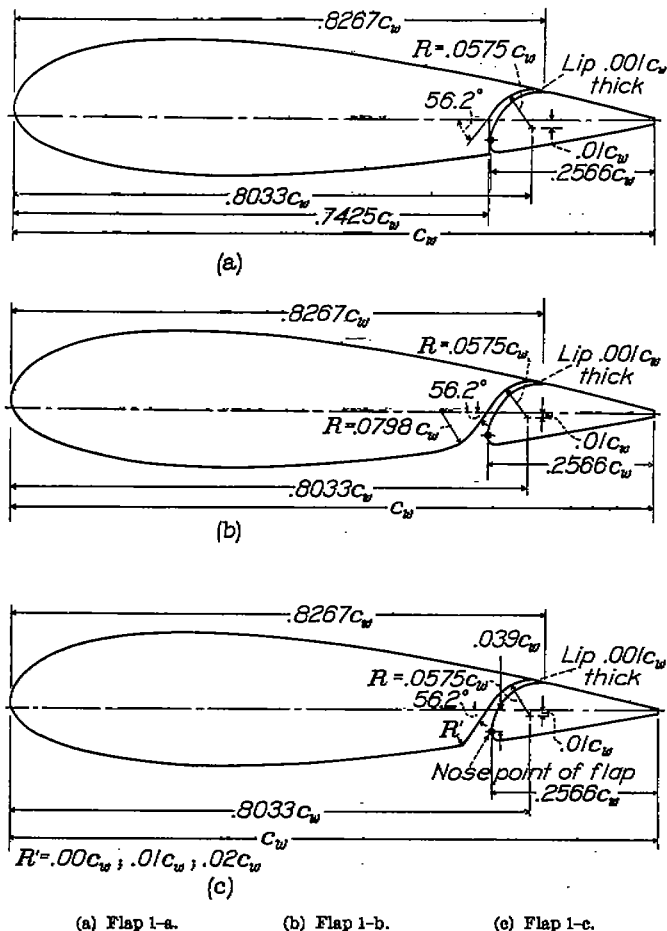


FIGURE 1.—Sections of N. A. C. A. 23021 airfoil with arrangements of slotted flap 1.

and high lift coefficients for take-off. This slot shape was also used in combination with both flaps and is shown in figures 1 (b) and 2 (b). Slot shape c was especially designed so that a door could be used to close the break in the lower surface of the wing with the flap neutral. This slot shape was used only in combination with flap 1 and was similar to shape b except for the entry radius. Slot shape c_0 has a sharp entry, and shapes c_1 and c_2 have entry radii 1 and 2 percent of the wing chord, respectively. All the slots were designed to be sealed by the slot lip at the exit on the upper surface of the wing with the flaps neutral.

The models were made to a tolerance of ± 0.015 inch.

TESTS

The models were mounted in the closed test section of the N. A. C. A. 7-by 10-foot wind tunnel so that they completely spanned the jet except for small clearances at each end. (See references 1 and 4.) The main airfoil was rigidly attached to the balance frame by torque tubes, which extended through the upper and the lower boundaries of the tunnel. The angle of attack of the model was set from outside the tunnel by rotating the torque tubes with a calibrated drive. Approximately two-dimensional flow is obtained with this type of installation and the section characteristics of the model under test can be determined.

A dynamic pressure of 16.37 pounds per square foot was maintained for most of the tests, corresponding to a velocity of 80 miles per hour under standard atmospheric

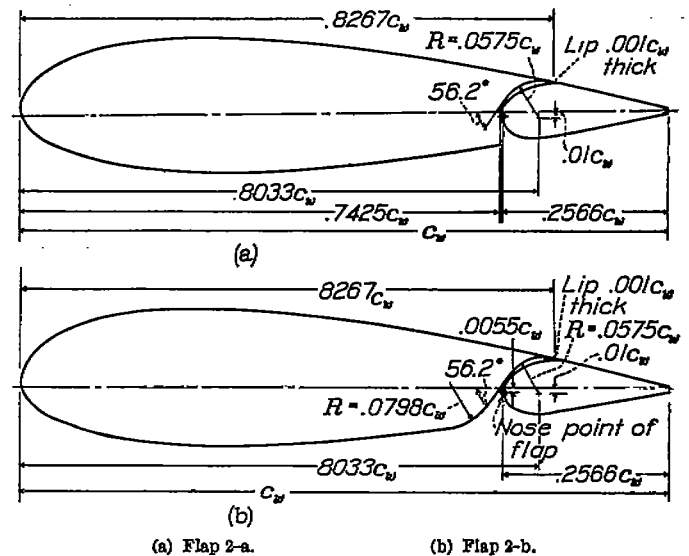


FIGURE 2.—Sections of N. A. C. A. 23021 airfoil with arrangements of slotted flap 2.

conditions and to an average test Reynolds Number of about 2,190,000. Because of the turbulence in the wind tunnel, the effective Reynolds Number R_e (reference 5) was approximately 3,500,000. For all tests, R_e is based on the chord of the airfoil with the flap retracted and on a turbulence factor of 1.6 for the tunnel.

Plain airfoil.—Tests were first made of the plain airfoil over the complete angle-of-attack range from -6° to the stall. In addition to this test, scale-effect tests were made of maximum lift coefficient over the range available in the 7-by 10-foot wind tunnel.

Slotted flaps.—With each slotted-flap arrangement, tests were made to determine the effect on minimum drag of the breaks in the wing lower surface at the slot entrance with the flap retracted. Tests were also made to determine the effect of the flap hinges with the flaps in their retracted positions. The tests of slotted flaps 1-a, 1-b, 2-a, and 2-b consisted in surveys of flap

position and deflection to determine the optimum path of the flap from a consideration of low drag throughout the complete lift range and of the highest maximum lift for each flap deflection. Tests were made of slotted flaps 1-c₀, 1-c₁, and 1-c₂ along the optimum path as determined for slotted flap 1-b. Data were obtained for all tests throughout the angle-of-attack range from -6° to the stall at 10° increments of flap deflection from 0° to 60°. No data were obtained above the stall because of the unsteady conditions of the model. Lift, drag, and pitching moments were measured for all positions of the flap over the complete angle-of-attack range tested.

Scale-effect tests of maximum lift were also made of slotted flap 2-b at the optimum position for maximum lift with the 50° flap deflection.

RESULTS AND DISCUSSION
COEFFICIENTS

All test results are given in standard section non-dimensional coefficient form corrected as explained in reference 1.

- c_l , section lift coefficient (l/qc_w).
- c_{d_0} , section profile-drag coefficient (d_0/qc_w).
- $c_{m(a.c.)_0}$, section pitching-moment coefficient about aerodynamic center of plain airfoil ($m_{(a.c.)_0}/qc_w^2$).

where

- l is section lift.
- d_0 , section profile drag.
- $m_{(a.c.)_0}$, section pitching moment.
- q , dynamic pressure ($1/2 \rho V^2$).
- c_w , chord of basic airfoil with the flap fully retracted.

and

- α_0 is angle of attack for infinite aspect ratio.
- δ_f , flap deflection.

PRECISION

The accuracy of the various measurements in the tests is believed to be within the following limits:

α_0	$\pm 0.1^\circ$
$c_{l_{max}}$	± 0.03
$c_{m(a.c.)_0}$	± 0.003
$c_{d_{0min}}$	± 0.0003
$c_{d_0(c_f=1.0)}$	± 0.0006
$c_{d_0(c_f=2.5)}$	± 0.002
δ_f	$\pm 0.2^\circ$
Flap position	$\pm 0.001c_w$

No corrections for flap-hinge fittings have been applied to the data because no effect could be measured with the flaps neutral. No attempt was made to determine the effect of the hinges with the flaps deflected because their effect was believed to be small and because of the great number of tests required. It is believed that the relative merits of the various flaps

are not appreciably affected because the same hinge fittings were used with all the airfoil-flap combinations.

PLAIN AIRFOIL

Aerodynamic characteristics.—The complete section aerodynamic characteristics of the plain N. A. C. A. 23021 airfoil are given in figure 3. Comparison with previously published data obtained from tests of a finite-span model and corrected to infinite aspect ratio

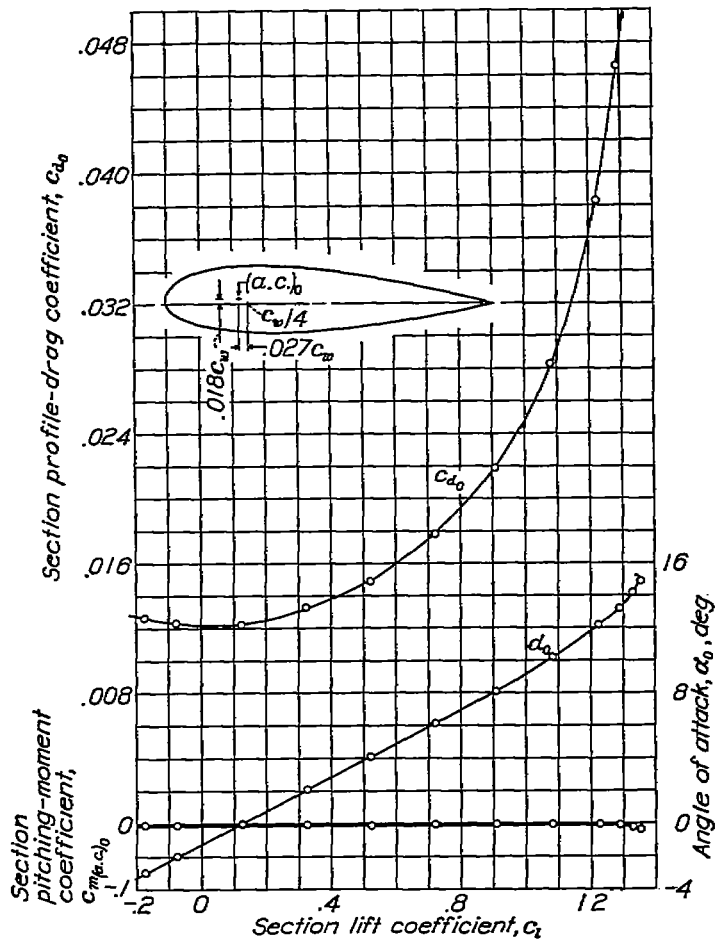


FIGURE 3.—Section aerodynamic characteristics of N. A. C. A. 23021 plain airfoil.

(reference 5) shows insignificant differences in the results. The slope of the lift curve and the values of the minimum drag coefficient are slightly higher for the present tests than for some of the results at a considerably higher Reynolds Number given in reference 5. The pitching-moment coefficient and the vertical location of the aerodynamic center above the chord line are slightly lower. The chordwise location of the aerodynamic center is the same for both sets of data. These differences are about the same as those observed between the results of previous two- and three-dimensional-flow tests of the N. A. C. A. 23012 airfoil (reference 1). The data for the N. A. C. A. 23021 airfoil given herein are directly comparable with the data for the N. A. C. A. 23012 (references 1, 2, and 3). When comparisons with other airfoils are made, it should be remembered

that no correction for tunnel effect has been applied to these data except for the lift, as explained in reference 1.

Effect on profile drag of breaks in surface of airfoil at slot entrance.—The effects of the breaks in the lower surface of the airfoil with the flaps undeflected are shown in figure 4. No measurable effect was evident from the breaks caused by the thickness of the slot lip in the upper surface of the airfoil. The increment of profile-drag coefficient, Δc_{d_0} , was smallest for slotted flap 1-a; Δc_{d_0} varied from 0.0002 at zero lift to 0.0006 at a lift coefficient of 1.0. Slotted flap 2-a had a constant increment of profile-drag coefficient of 0.0006

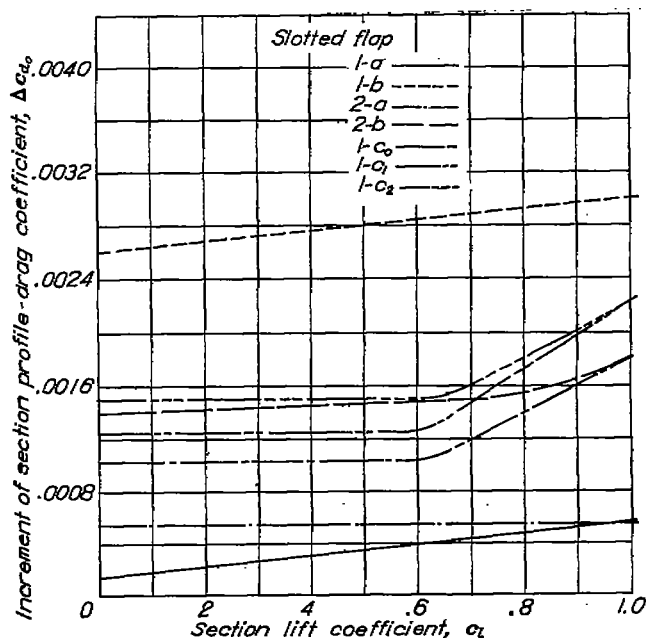


FIGURE 4.—Effect of slot openings in lower surface of airfoil on profile-drag coefficient. $\delta_1, 0^\circ$.

for all lift coefficients from zero lift to a lift coefficient of 1.0. Slotted flaps 1-c₀ and 1-c₁ gave approximately constant increments of profile-drag coefficient of about 0.0010 and 0.0012, respectively, up to a lift coefficient of 0.6, beyond which the increments increased to 0.0018 and 0.0022 at a lift coefficient of 1.0. Slotted flaps 1-c₂ and 2-b gave about the same increment of profile-drag coefficient, 0.0014 to 0.0015, for lift coefficients less than 0.6, beyond which the increments increased to 0.0022 and 0.0018, respectively, at a lift coefficient of 1.0. Slotted flap 1-b was inferior to all other arrangements, the increment of profile-drag coefficient increasing nearly linearly from 0.0026 at zero lift to 0.0030 at a lift coefficient of 1.0.

It is probable that a door could be fitted to any of the arrangements in such a manner as to seal the break in the airfoil lower surface without measurably increasing the profile-drag coefficient of the wing with the flap neutral over that of the plain wing.

SLOTTED-FLAP ARRANGEMENT

Determination of optimum arrangements for maximum lift.—The data presented in this section are the results of the maximum-lift investigation of the various flap-and-slot combinations in which the flap, at a given deflection, was located at points over a considerable area with respect to the main airfoil. The data are presented as contours of the position of the nose point of the flap for a given lift coefficient. The nose point of the flap is defined as the point of tangency of a line drawn perpendicular to the airfoil chord and tangent to the leading-edge arc of the flap when neutral, as shown in figures 1 and 2.

The complete maximum-lift data for slotted flaps 1-a, 1-b, 2-a, and 2-b deflected 10°, 20°, 30°, 40°, 50°, and 60° are given in figures 5 to 8, respectively. An inspection of these figures shows that the contours are not closed with all combinations for flap deflections less than 30°. The position for maximum lift coefficient is not very critical and only a sufficient number of positions were taken to cover any practical path along which the flap is likely to be operated. Furthermore, it is probable that the optimum flap position for these deflections will be chosen from a consideration of drag and ease of mechanical operation.

The position of the flaps for maximum lift coefficient becomes much more critical for flap deflections from 40° to 60°. The maximum lift coefficient was obtained for slotted flaps 1-a and 1-b with the flap deflected 60° and the nose point 1.5 percent of the wing chord directly below the slot lip. With slotted flaps 2-a and 2-b, the maximum lift coefficient at 50° flap deflection was obtained with the flap nose point about 2.5 percent of the wing chord directly below the slot lip.

From these contours, it should be possible for the designer to choose the best path for the flap to follow from a consideration of maximum lift coefficient alone. If, from structural considerations, it is not possible to use the best aerodynamic path, the loss caused by using a compromise path can be immediately evaluated. Complete section aerodynamic characteristics of selected optimum arrangements for each flap deflection are given in a later section of this report.

Determination of optimum arrangements for profile drag.—Optimum positions of the several flaps for the conditions of low drag for take-off and initial climb to clear an obstacle were determined. The sole criterion for a given lift coefficient is the drag coefficient.

The most important single factor in unassisted take-off distance is the value of the lift coefficient for take-off because the higher the lift coefficient, the lower the take-off speed and, other conditions being equal, the shorter the distance required to clear a given obstacle.

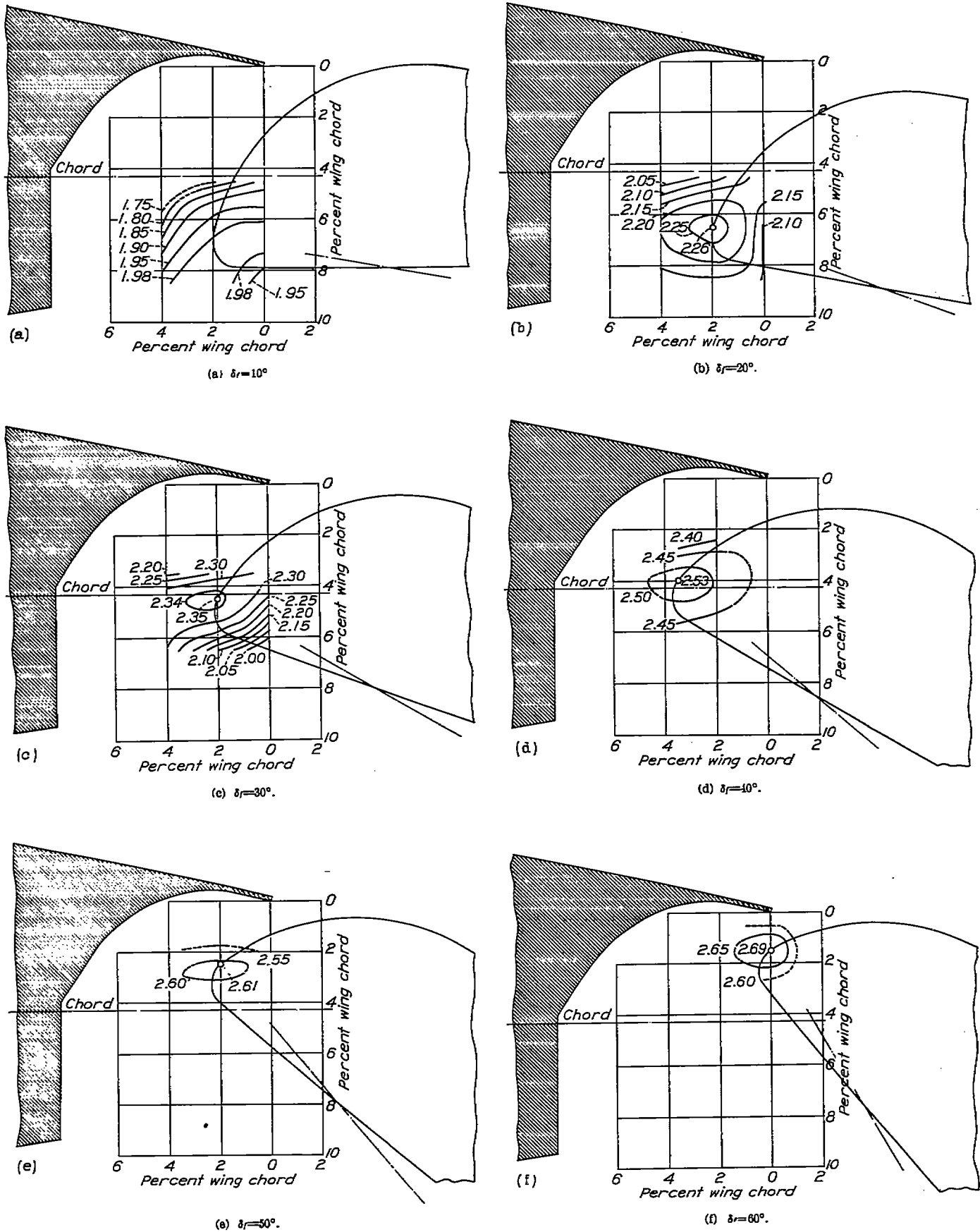
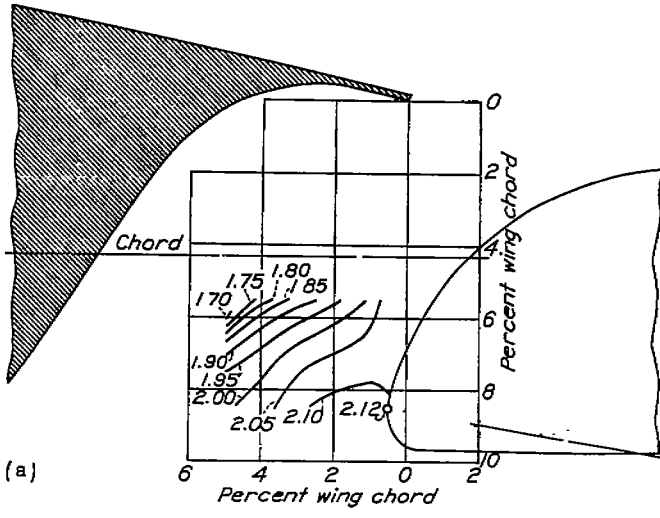
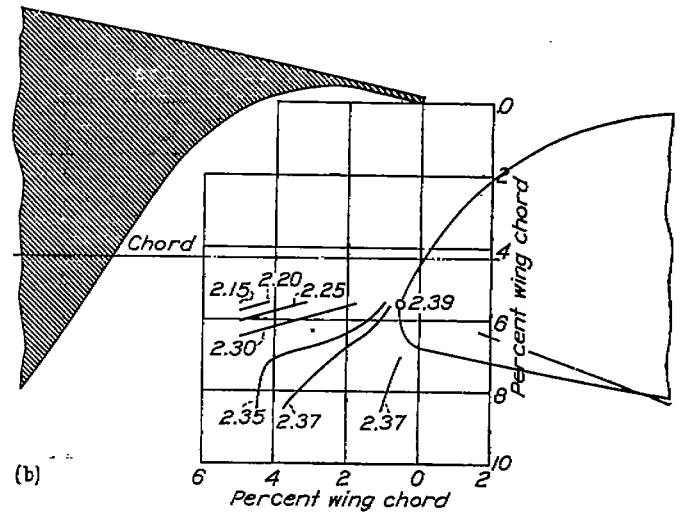


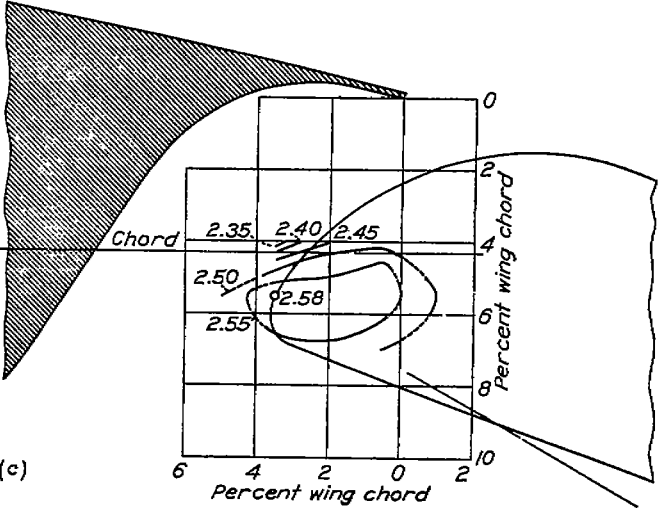
FIGURE 5.—Contours of flap location for $c_{l,max}$. Slotted flap 1-a.



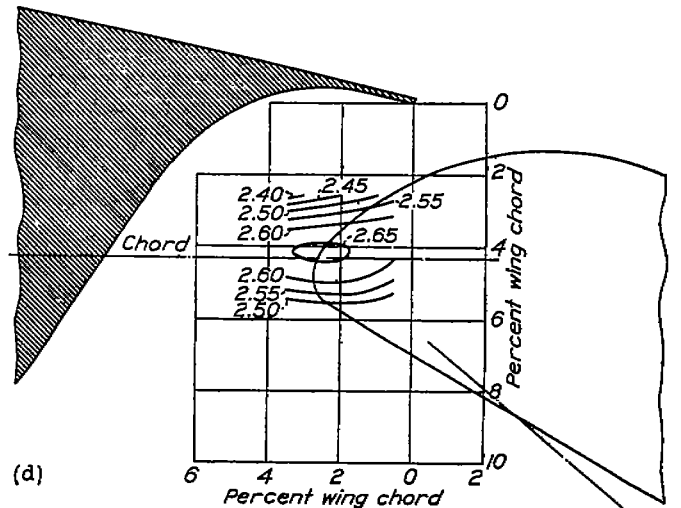
(a) $\delta_f = 10^\circ$.



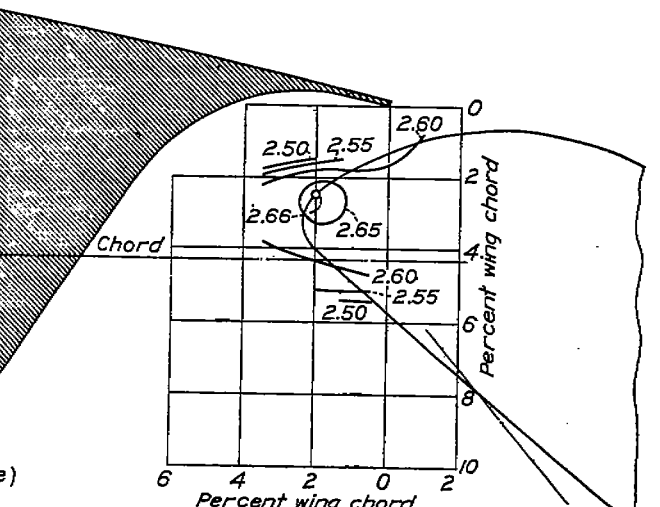
(b) $\delta_f = 20^\circ$.



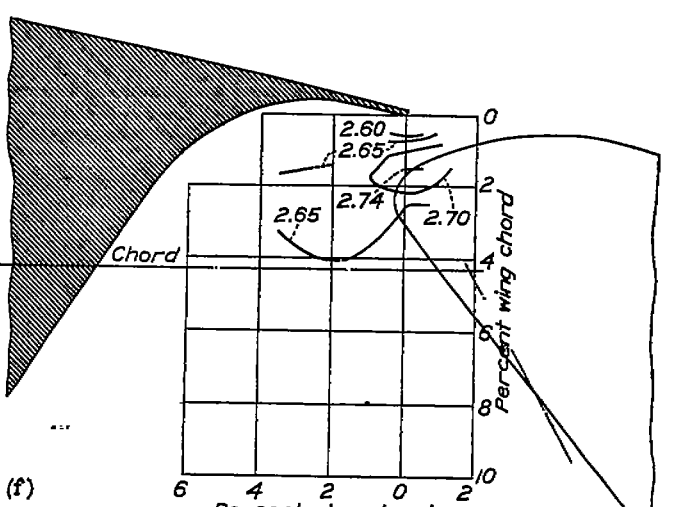
(c) $\delta_f = 30^\circ$.



(d) $\delta_f = 40^\circ$.

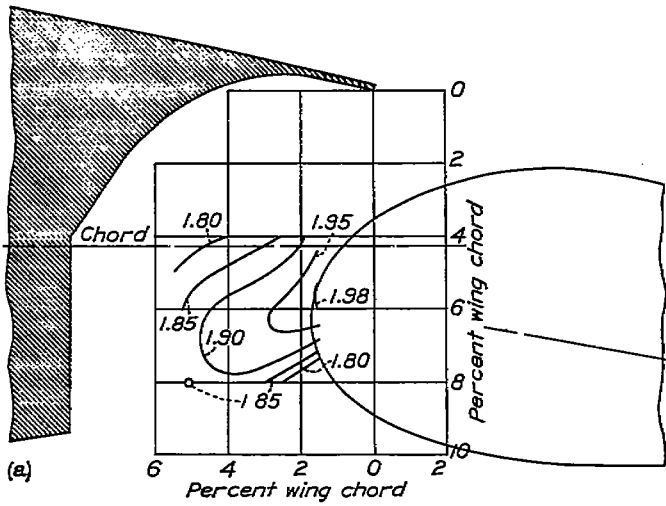


(e) $\delta_f = 50^\circ$.

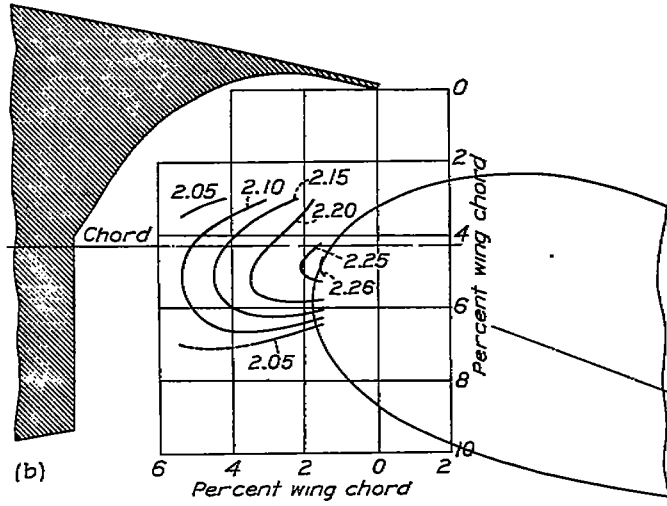


(f) $\delta_f = 60^\circ$.

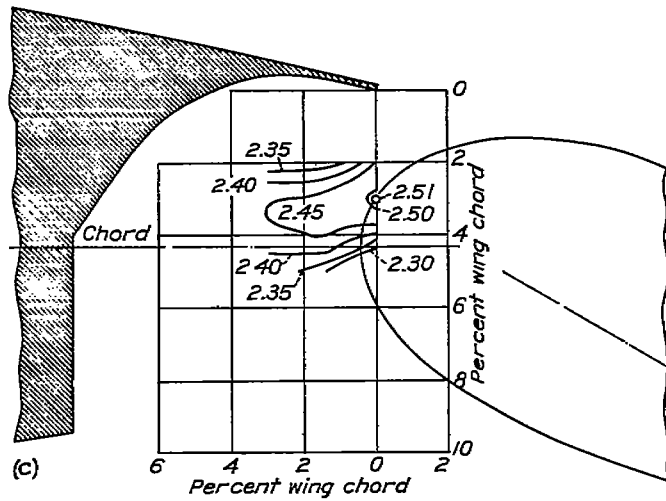
FIGURE 6.—Contours of flap location for $c_{l_{max}}$. Slotted flap 1-b.



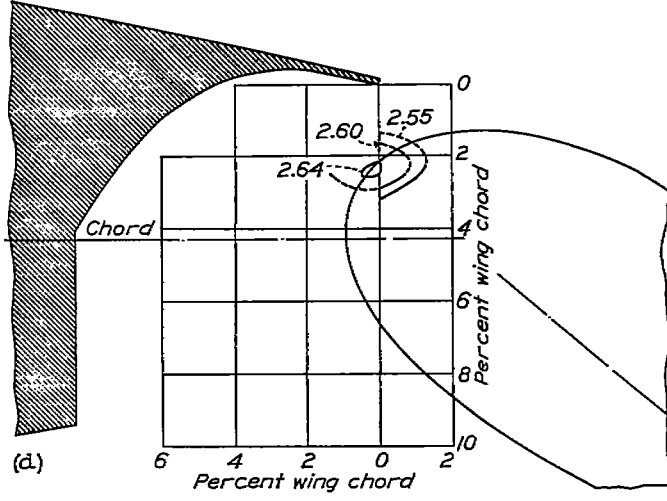
(a) $\delta_f = 10^\circ$.



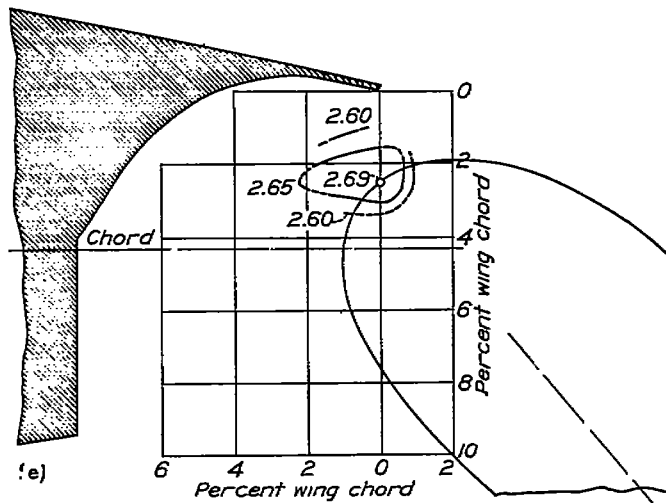
(b) $\delta_f = 20^\circ$.



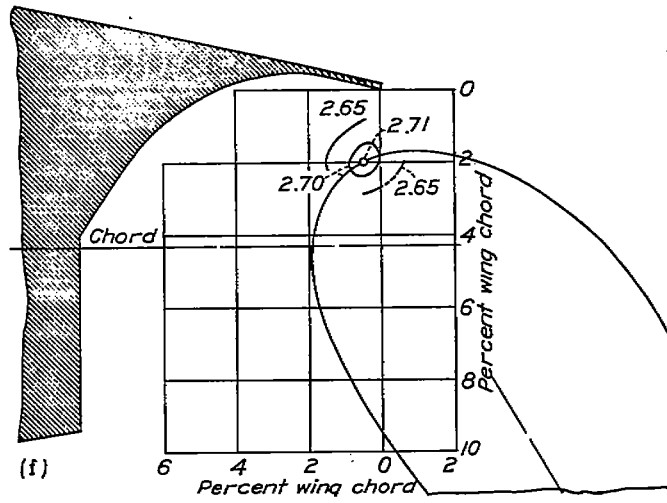
(c) $\delta_f = 30^\circ$.



(d) $\delta_f = 40^\circ$.



(e) $\delta_f = 50^\circ$.



(f) $\delta_f = 60^\circ$.

FIGURE 7.—Contours of flap location for $c_{l_{max}}$. Slotted flap 2-a.

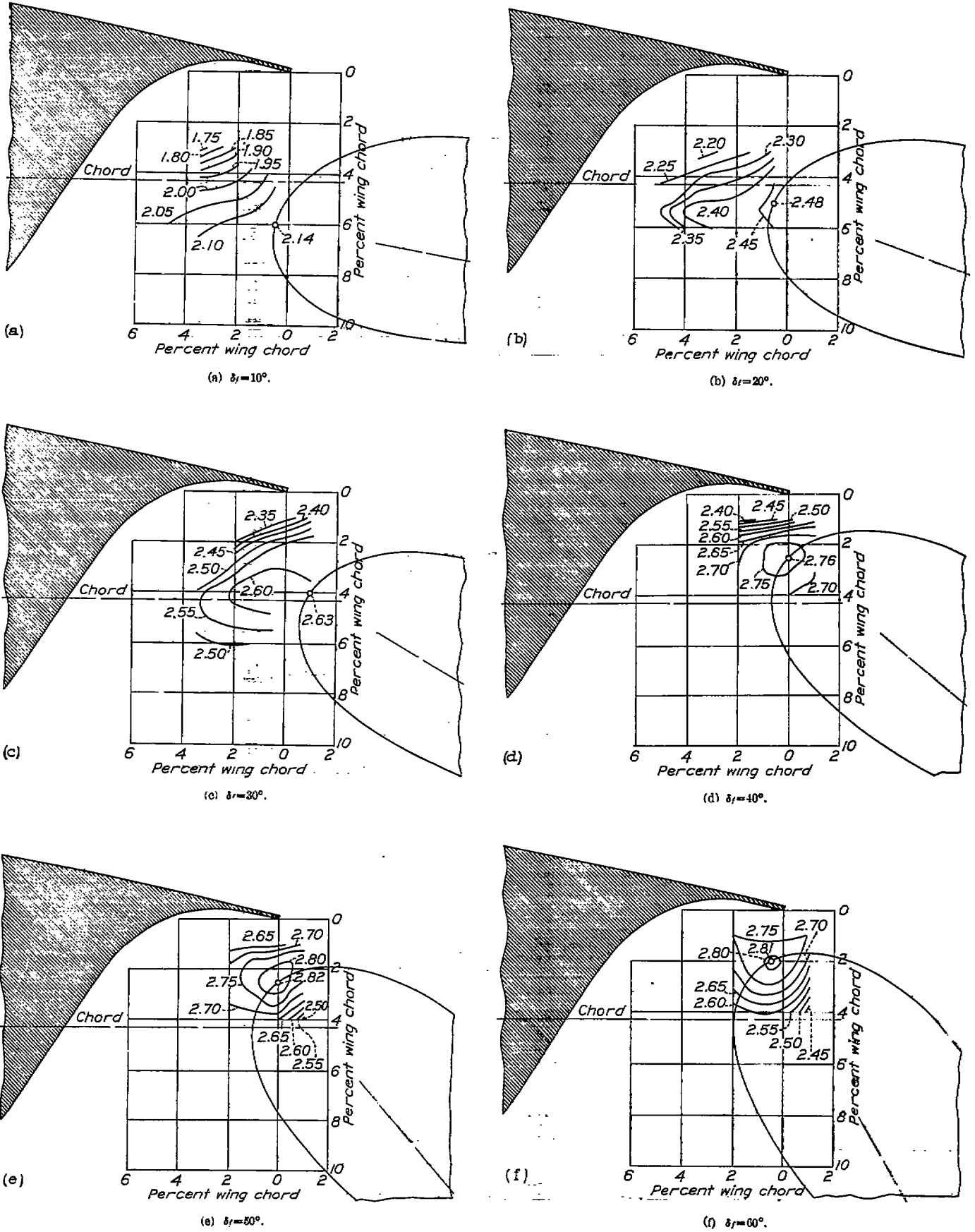


FIGURE 8.—Contours of flap location for $c_{l,max}$. Slotted flap 2-b.

The limiting conditions are the power available to overcome the drag at the higher lift coefficients and the excess available lift required from considerations of safety. The data are given, therefore, as contours of the nose position of the flap for constant drag coefficients at certain selected lift coefficients, $c_l=1.0, 1.5, 2.0,$ and $2.5,$ and for flap deflections that cover the range for which the drag coefficient is decreased by deflecting the flap.

The complete drag data for slotted flaps 1-a, 1-b,

Section aerodynamic characteristics of selected optimum arrangements.—The complete section aerodynamic characteristics of selected optimum arrangements of slotted flaps 1-a, 1-b, 2-a, and 2-b are given in figures 13 to 16, respectively. The optimum arrangements were chosen from a consideration of low drag coefficients at the specified lift coefficients for flap deflections from 10° to 30° and from a consideration of maximum lift coefficient alone for flap deflections from 40° to 60° . In addition to the optimum arrangements,

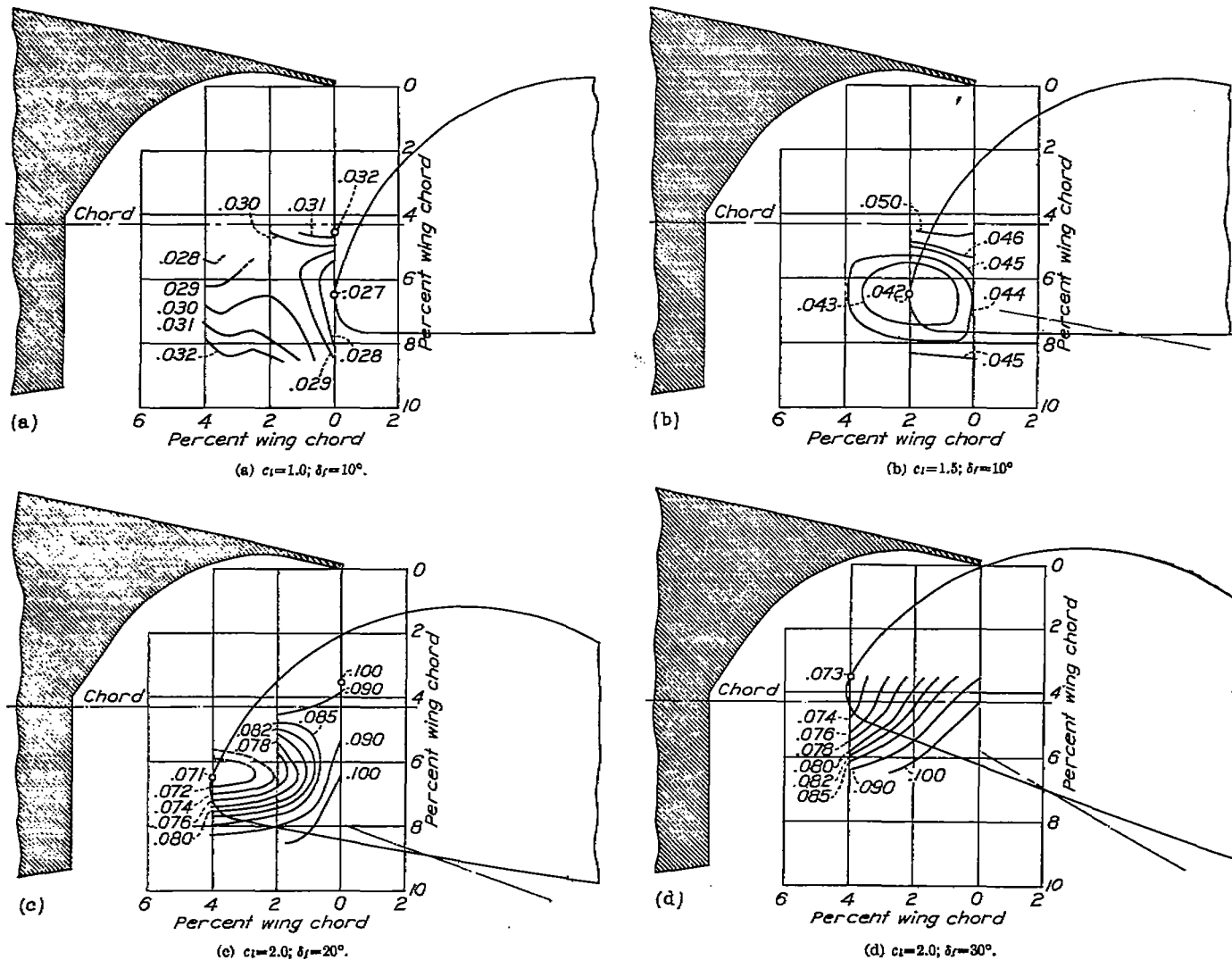


FIGURE 9.—Contours of flap location for c_{d_p} . Slotted flap 1-a.

2-a, and 2-b are given in figures 9 to 12, respectively. Where the minimum drag coefficients were approximately the same for a given lift coefficient at two flap settings, both sets of data are given. From these data, optimum paths for the nose points of the several flaps may be chosen from a consideration of drag coefficients at the various lift coefficients. If it is structurally impossible to follow the optimum path, the additional drag coefficient caused by the deviation will be available. Insufficient data were obtained to close all the contours, but most of the practicable arrangements are believed to be within the range covered.

data are also given for certain arrangements that appear structurally simpler. A table included in each figure shows the nose position of the flap for the various deflections and the points are plotted on the diagrams. The selected optimum path referred to hereinafter is shown by the broken line through the points and is a compromise between aerodynamic and structural considerations. The aerodynamic characteristics shown in these figures are typical; complete data for other positions of the various flaps at the several flap deflections are available upon request.

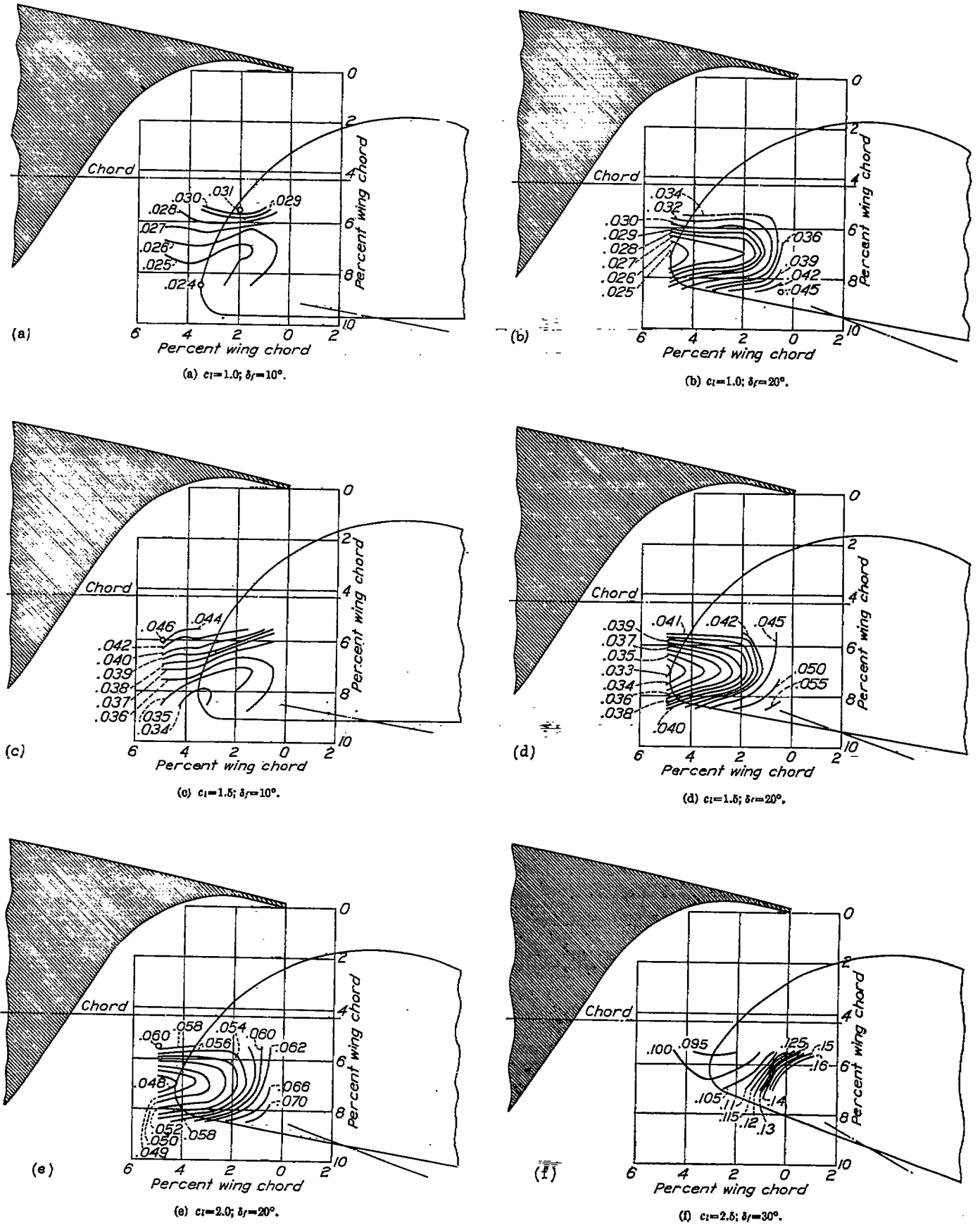
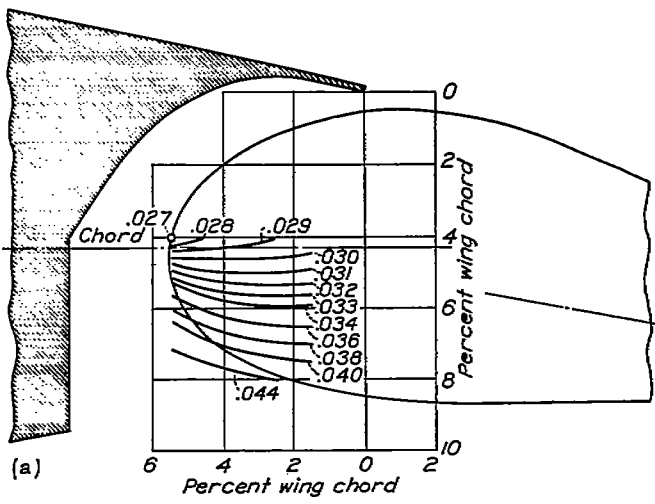
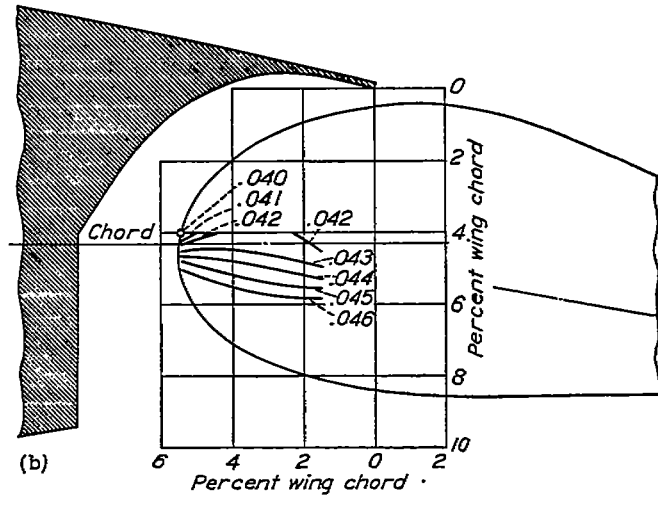


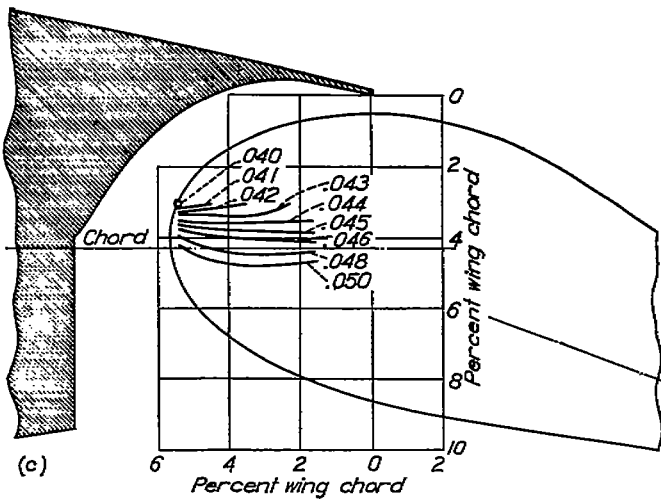
FIGURE 10.—Contours of flap location for c_{l_f} . Slotted flap 1-b.



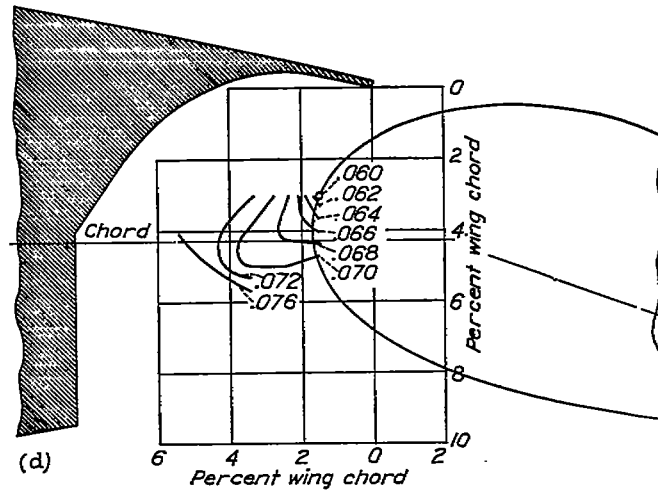
(a) $c_l=1.0; \delta_f=10^\circ$.



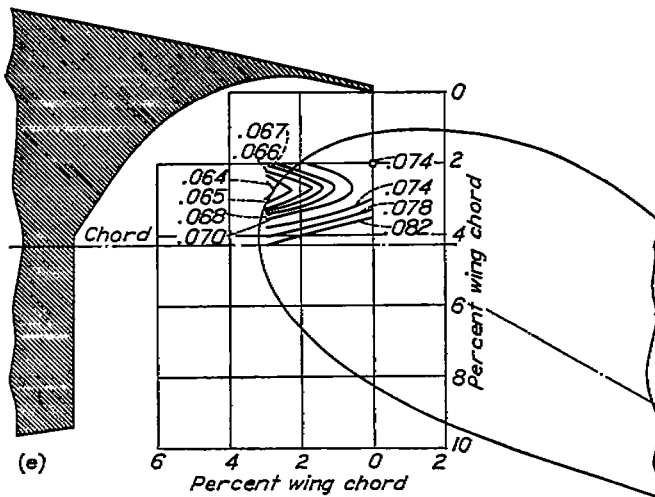
(b) $c_l=1.5; \delta_f=10^\circ$.



(c) $c_l=1.5; \delta_f=20^\circ$.



(d) $c_l=2.0; \delta_f=20^\circ$.



(e) $c_l=2.0; \delta_f=30^\circ$.

FIGURE 11.—Contours of flap location for c_{d_4} . Slotted flap 2-a.

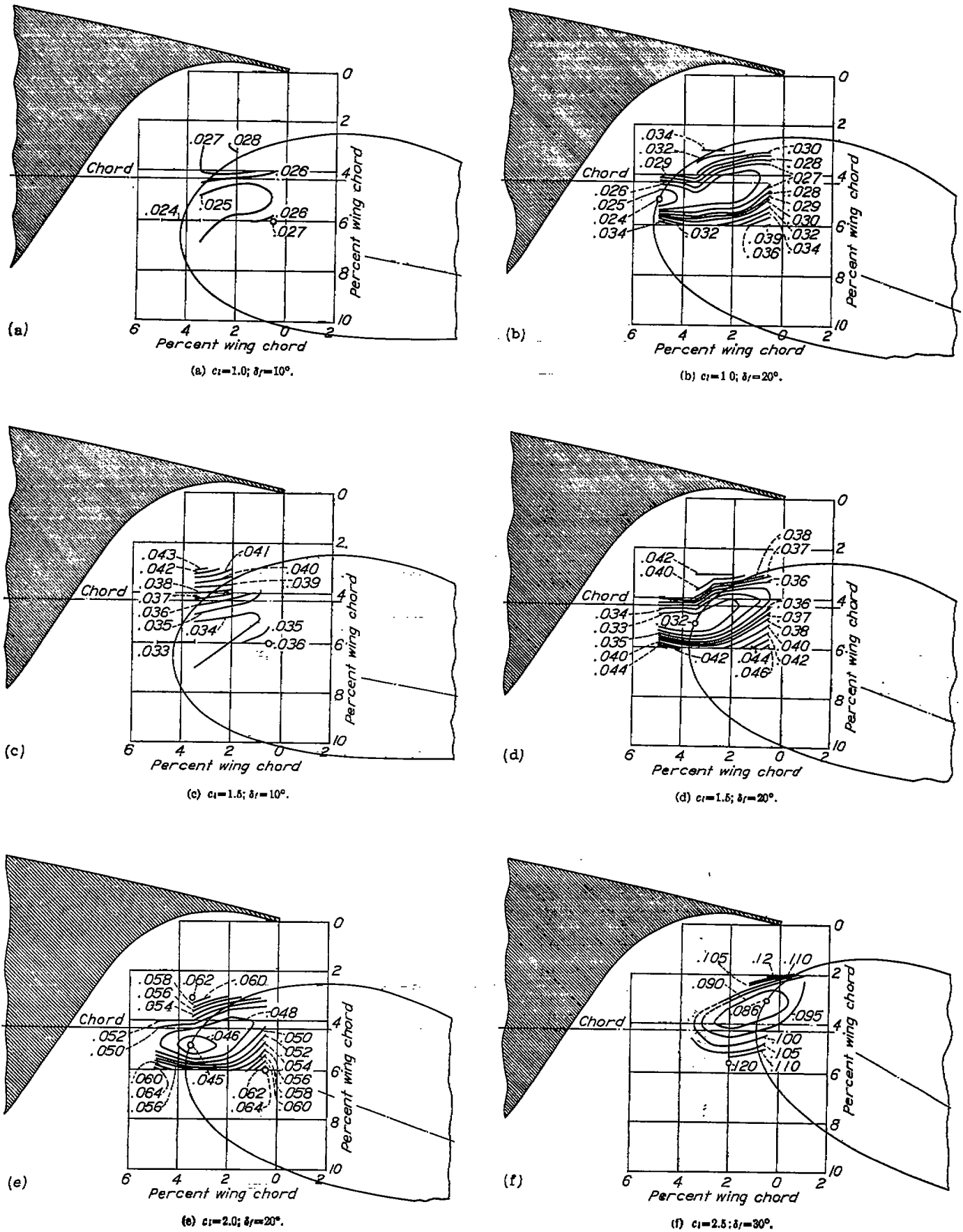


FIGURE 12.—Contours of flap location for $c_{l\alpha}$. Slotted flap 2-b.

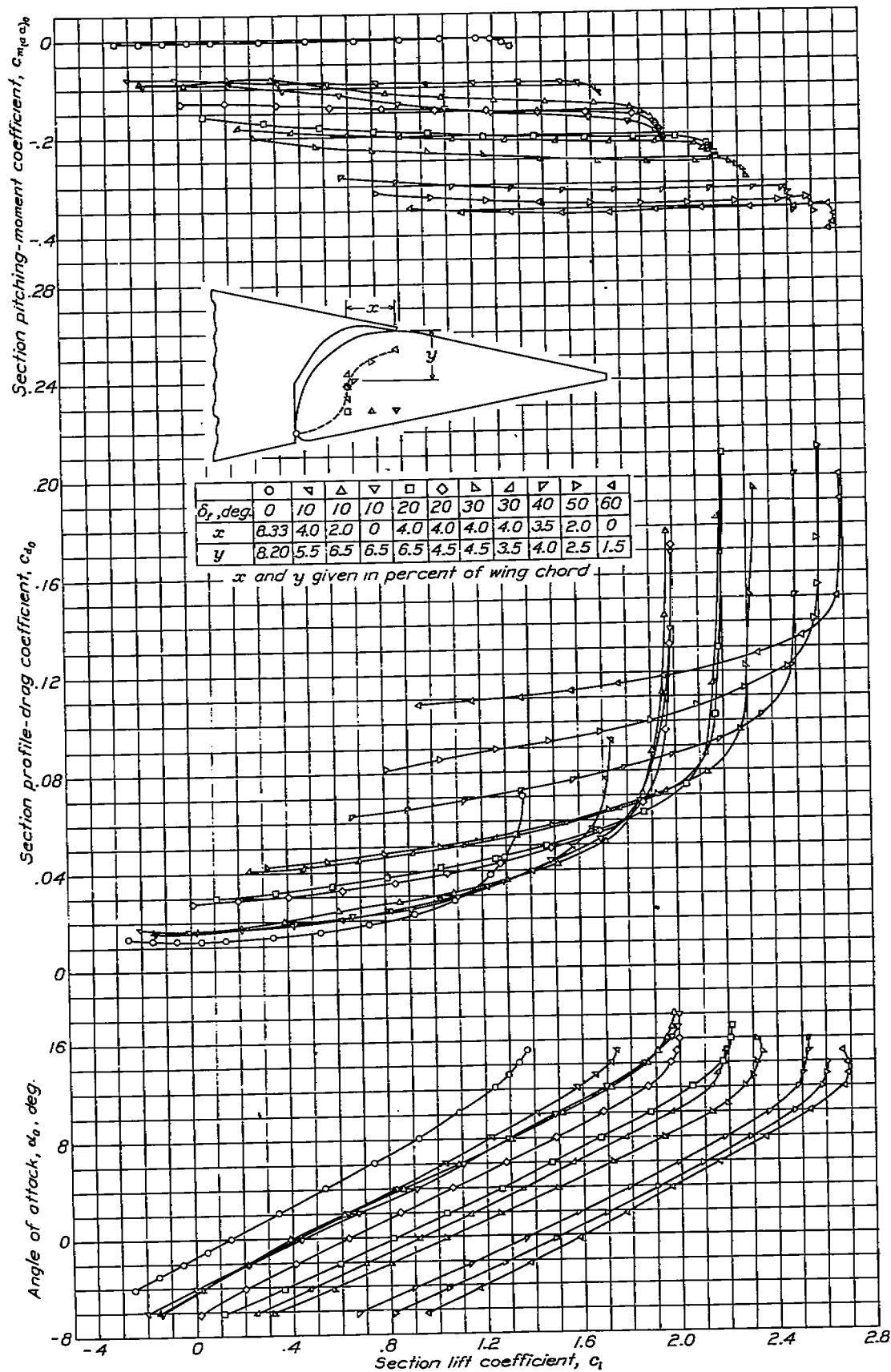


FIGURE 13.—Section aerodynamic characteristics of N. A. C. A. 23021 airfoil with slotted flap 1-a.

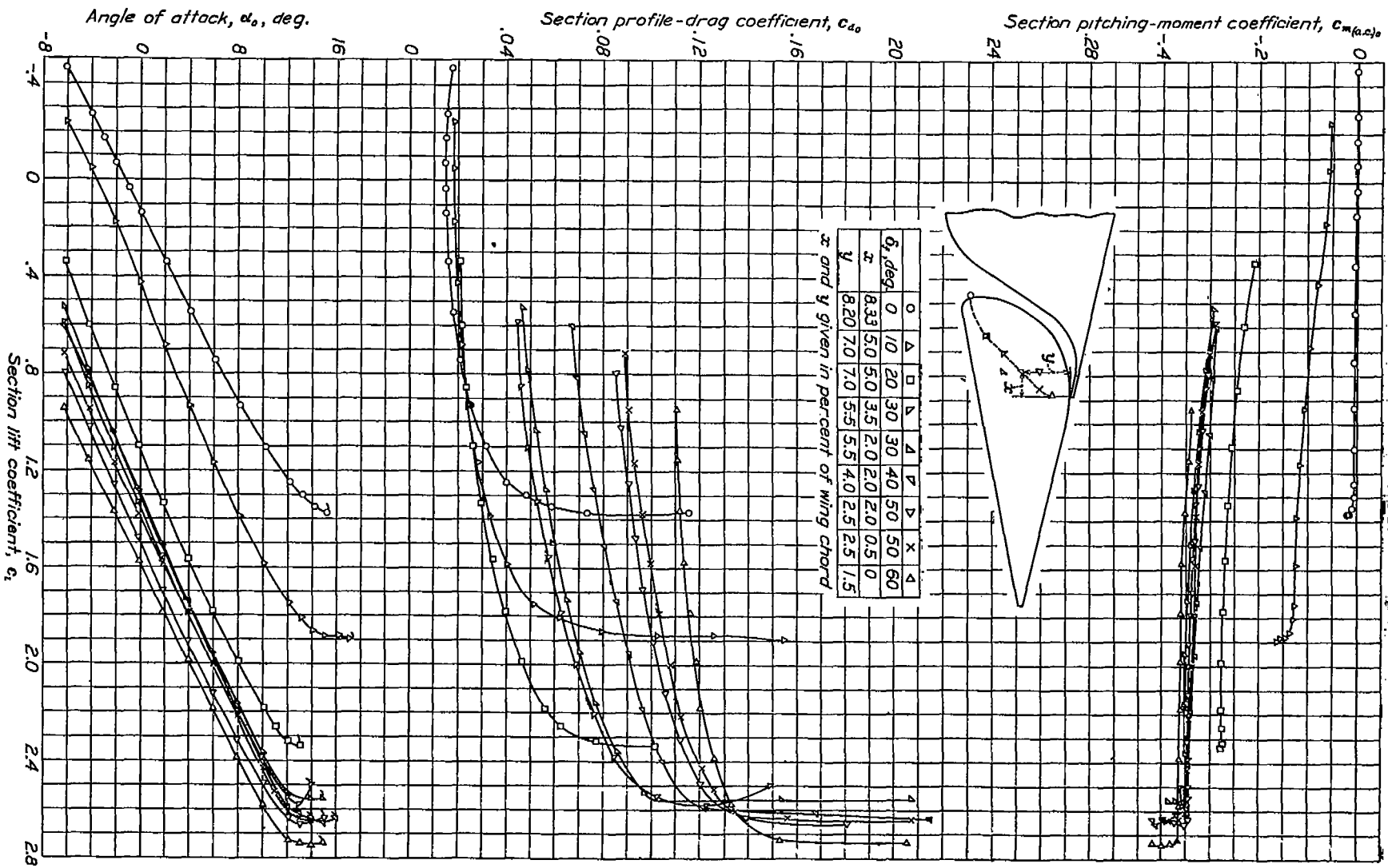


FIGURE 14.—Section aerodynamic characteristics of N. A. A. O. A. 28021 airfoil with slotted flap 1-b.

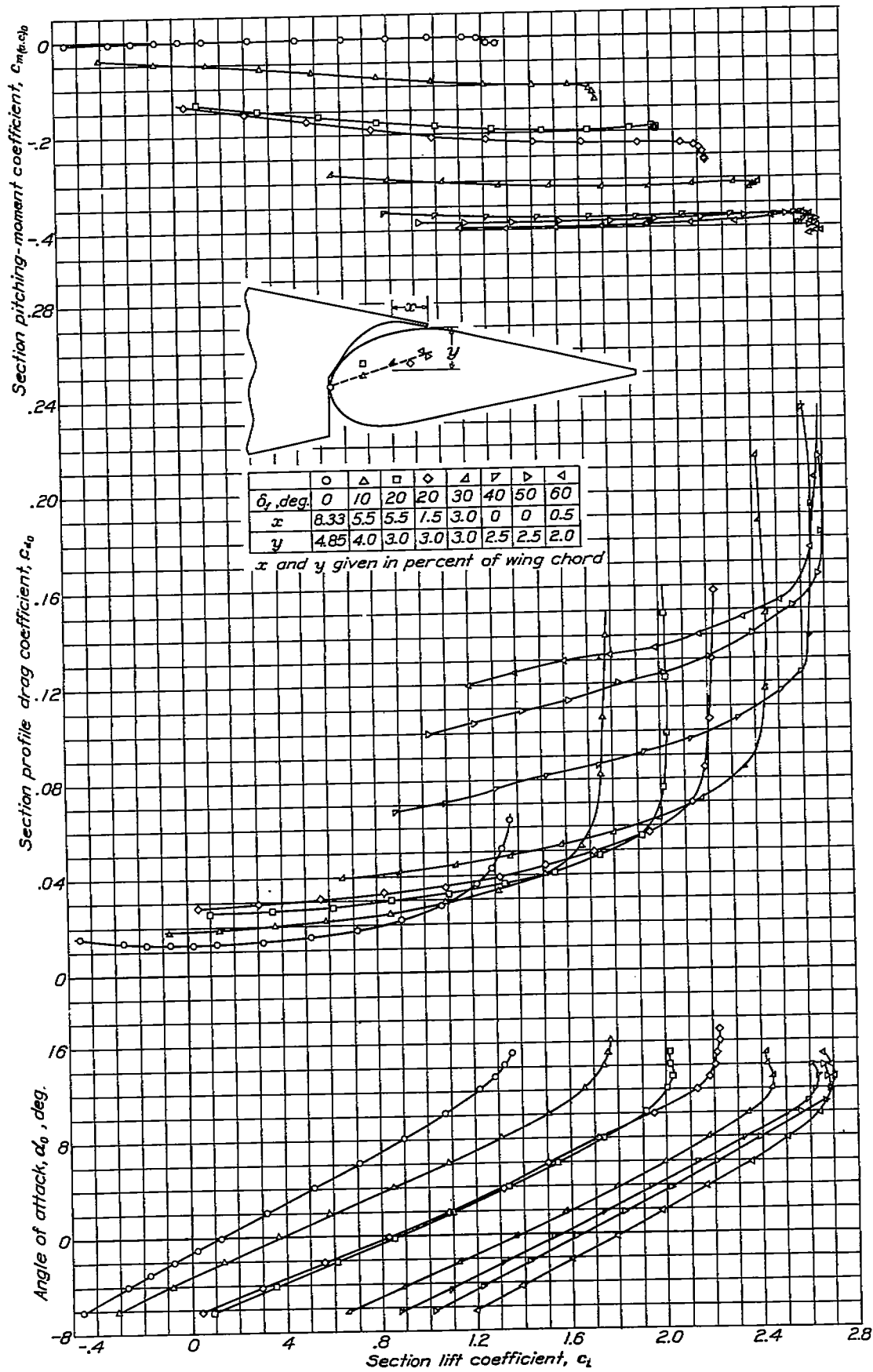


FIGURE 15.—Section aerodynamic characteristics of N. A. C. A. 23021 airfoil with slotted flap 2-a.

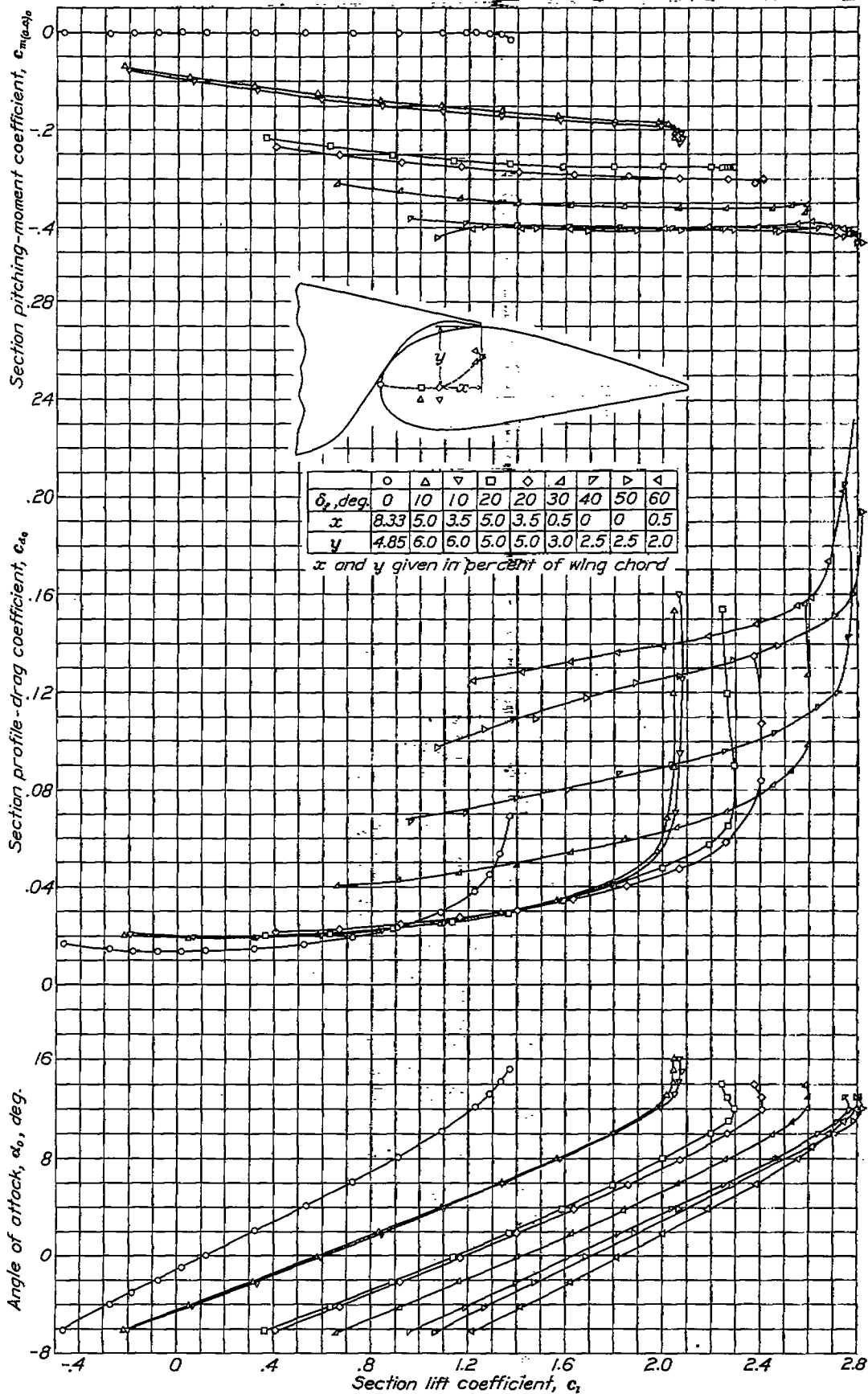


FIGURE 16.—Section aerodynamic characteristics of N. A. C. A. 23021 airfoil with slotted flap 2-b.

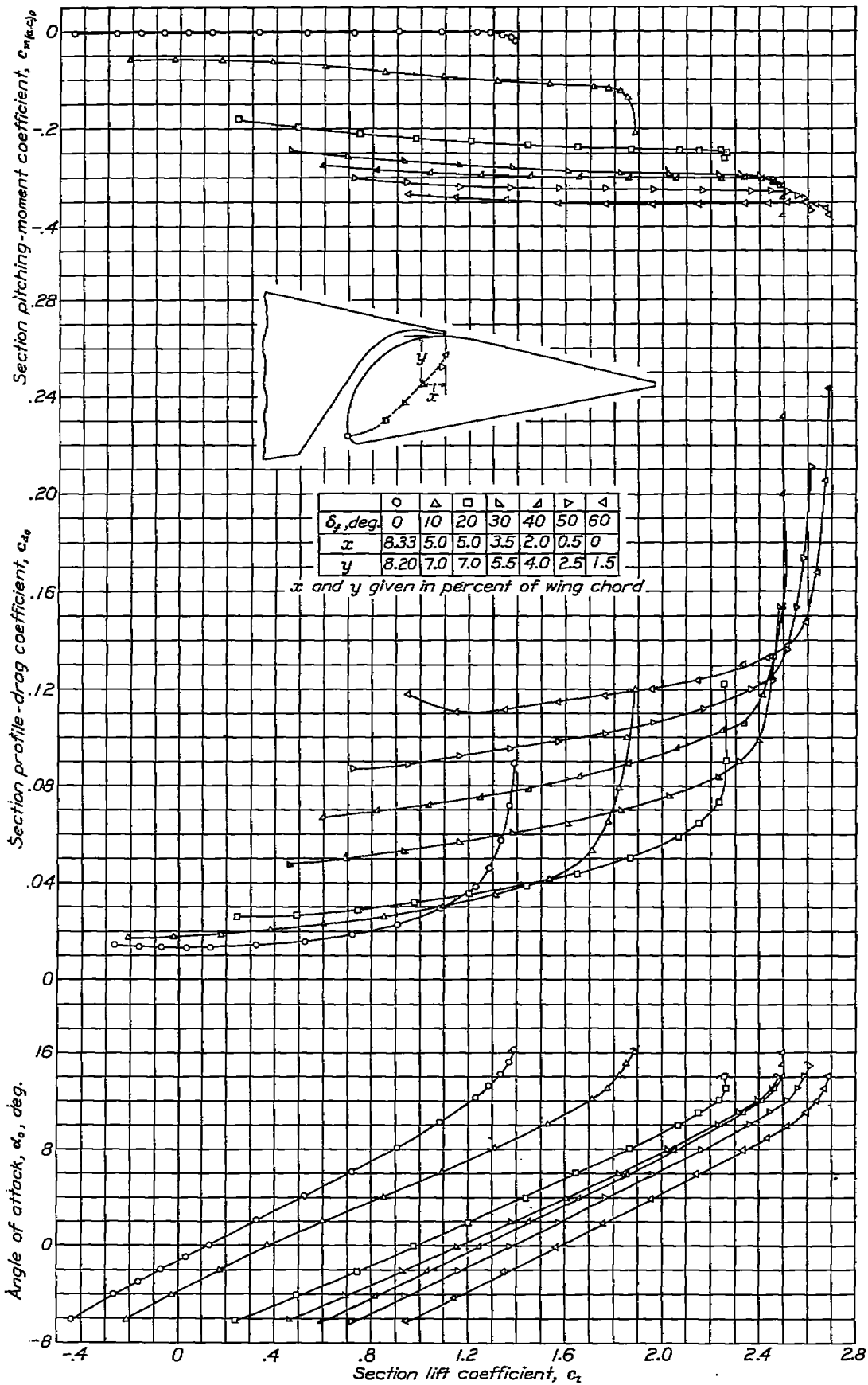


FIGURE 17.—Section aerodynamic characteristics of N. A. C. A. 23021 airfoil with slotted flap 1-c₁.

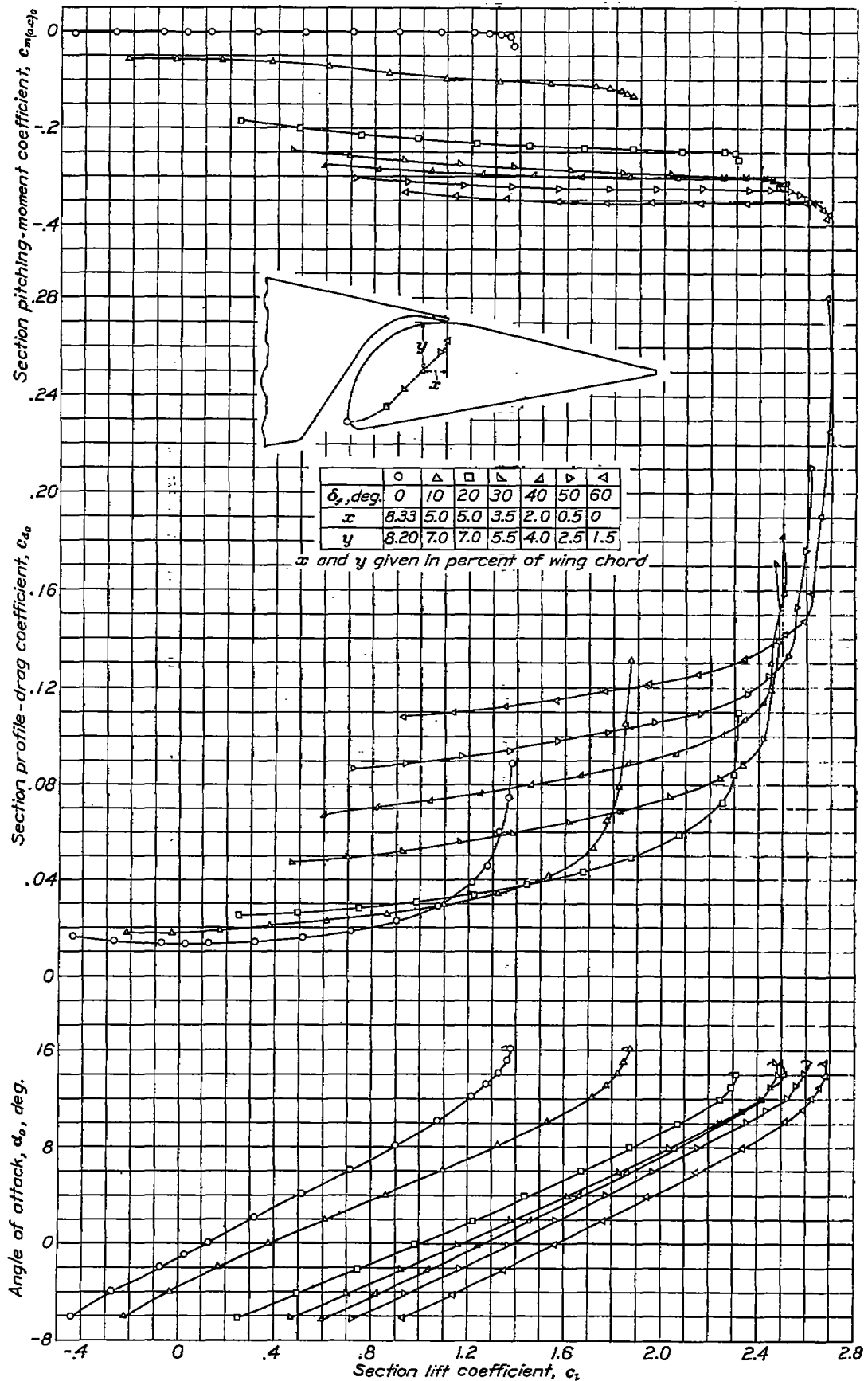


FIGURE 18.—Section aerodynamic characteristics of N. A. C. A. 23021 airfoil with slotted flap 1-0.

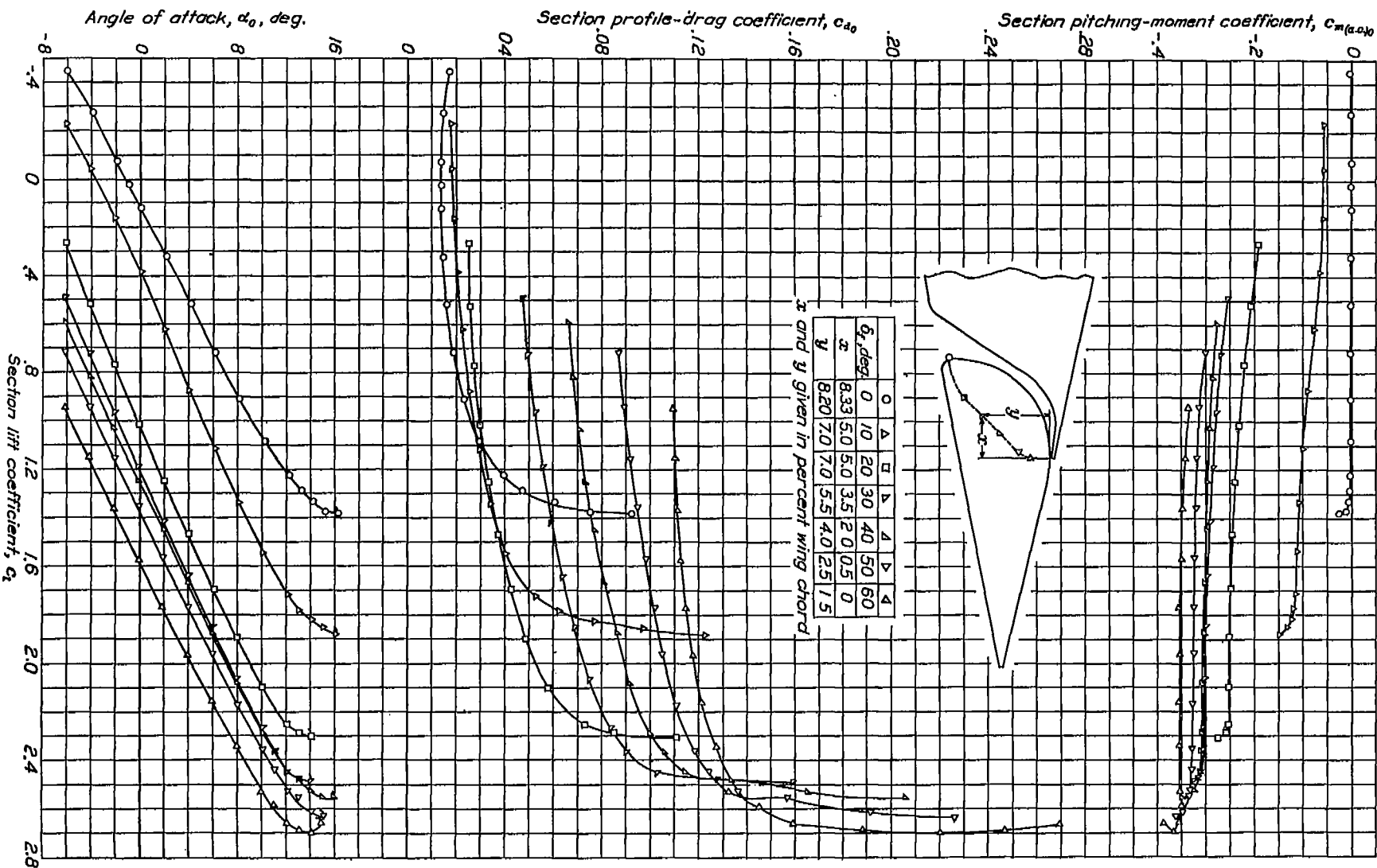


FIGURE 19.—Section aerodynamic characteristics of N. A. C. A. 23021 airfoil with slotted flap 1- ϵ_2 .

The complete section aerodynamic characteristics of slotted flaps 1-c₀, 1-c₁, and 1-c₂ are given in figures 17 to 19, respectively. These data are all that were obtained for these slotted flaps. The path of the flap nose used for all three arrangements was the same as for slotted flap 1-b.

Comparison of selected optimum arrangements.—In order to compare the drags of the various flap arrangements, envelope polars are given in figure 20 for the slotted-flap arrangements of figures 13 to 16. This figure shows slotted flap 2-b to be superior for take-off at any lift coefficient from 1.0 up to the maximum lift coefficient. Slotted flap 1-b is only slightly inferior to slotted flap 2-b over the same lift range. Slotted flaps 1-a and 2-a are both inferior to 1-b throughout the lift range from lift coefficients of 1.0 to that for maximum lift, flap 2-a being slightly superior to flap 1-a. A comparison of slotted flaps 1-b, 1-c₀, 1-c₁, and 1-c₂ for the take-off condition is given in figure 21 as envelope polars. Slotted flap 1-b, which has an 8-percent radius at the slot entry, is superior to the others. The slot entry with the sharp edge (slotted flap 1-c₀) appears to be the least desirable although there is little difference among the three.

For lift coefficients less than 1.0, the plain wing has lower drag coefficients than any of the arrangements with the flaps deflected; therefore, if a door were used to seal the break in the lower surface of the wing at the slot entrance, all the slotted-flap arrangements would be of equal merit for lift coefficients less than 1.0. The use of a door would probably be more complicated with slotted flaps 1-b and 2-b than with 1-c₀, 1-c₁, or 1-c₂; because of structural considerations, no definite conclusion can therefore be drawn as to which slotted flap would be superior. From a purely aerodynamic consideration, however, slotted flap 2-b is superior for conditions of take-off and initial climb to clear a given obstacle.

A comparison of slotted flaps 1-a, 1-b, 2-a, and 2-b as lift-increasing devices is shown in figure 22 where the increments of maximum lift coefficient $\Delta c_{l_{max}}$ are plotted against flap deflection when the flap is moved along the optimum path previously mentioned. Slotted flap 2-b is superior as a lift-increasing device, and the maximum increase in $\Delta c_{l_{max}}$ is obtained with a flap deflection of 50° with only a slight loss at a flap deflection of 60°. The other slotted-flap arrangements are all somewhat inferior to 2-b, the maximum lift coefficient being from 3 percent less for slotted flap 1-b to about 4 percent less for slotted flaps 1-a and 2-a.

The change in slot-entry radius had a negligible effect on the maximum increments of maximum lift coefficient as shown in figure 23, where $\Delta c_{l_{max}}$ is plotted against flap deflection for slotted flaps 1-b, 1-c₀, 1-c₁, and 1-c₂, all flaps being deflected along the optimum path selected for flap 1-b.

The scale effect for the range available in the 7- by

10-foot wind tunnel is shown in figure 24, where the $c_{l_{max}}$ for the plain airfoil and the $c_{l_{max}}$ for slotted flap 2-b at the optimum deflection ($\delta_f=50^\circ$) are plotted against effective Reynolds Number. A comparison of the two curves shows a slight increase in $\Delta c_{l_{max}}$ with an increase in scale but it is probable that, if the increment were considered to be independent of scale in applying the results at higher values of the Reynolds Number, the result would be conservative. It should be remembered, however, that the maximum lifts presented in this report are section, or infinite-aspect-ratio, characteristics and will not be realized on a finite-aspect-ratio wing except for one with an elliptic lift distribution.

A further comparison of the various slotted-flap arrangements is given in the following table:

Slotted flap	$c_{l_{max}}$	$c_{l_{max}}$	$c_{l_{max}}$	$c_{l_{max}}$	$c_{l_{max}}$	$(l/d)_{(0.9c_{l_{max}})}$	$c_{m_{max}}$
		$c_{d_{0_{min}}}$	$c_{d_{0_{(c_l=0.8)}}$	$c_{d_{0_{(c_l=0.6)}}$	$c_{d_{0_{(c_l=0.4)}}$		
None.....	1.35	111	108	98	85	32.4	-0.003
1-a.....	2.89	218	212	191	164	18.6	-0.360
1-b.....	2.74	185	180	165	146	19.1	-0.365
2-a.....	2.71	212	207	190	164	16.1	-0.325
2-b.....	2.82	207	208	196	161	16.3	-0.404
1-c ₀	2.69	204	199	182	165	18.2	-0.355
1-c ₁	2.69	200	196	170	165	17.5	-0.365
1-c ₂	2.69	197	192	176	164	18.5	-0.256

The maximum efficiency for a given landing speed will be obtained with the airfoil that gives the highest ratio of maximum lift coefficient to the drag coefficient for cruising. A comparison on this basis of the several slotted-flap arrangements shows slotted flap 1-a to be superior to any of the other arrangements for the conditions assumed. When the cruising speed is obtained at a lift coefficient of 0.6, flap 2-a is equally as good as 1-a, and 2-b is only slightly inferior to either. If a door were used to close the break in the lower surface of the wing when the flaps are neutral, the speed-range ratio ($c_{l_{max}}/c_{d_{0_{min}}}$) would be highest for slotted flap 2-b because it has the highest maximum lift coefficient. The optimum slotted flap from consideration of speed-range ratio will, therefore, depend upon whether a door is used to close the break in the lower surface of the wing with the flap neutral.

The ratio of lift to drag at $0.9c_{l_{max}}$, $(l/d)_{(0.9c_{l_{max}})}$, is a criterion of the maximum gliding angle; the lower the ratio, the steeper the angle of glide. The ratios tabulated in the table were obtained by dividing $0.9c_{l_{max}}$ with the respective flaps deflected 60°, by the drag coefficient at $0.9c_{l_{max}}$. Slotted flaps 2-a and 2-b will give the steepest gliding angle on this basis.

In order to control the glide-path angle, it is desirable to have available not only a low ratio of l/d at a high lift coefficient but also a high ratio of l/d . Slotted flap 2-b is superior in this respect, for the maximum lift is practically the same for flap deflections from 40° to 60° but the profile-drag coefficient for $\delta_f=40^\circ$ is only about one-half of its value for $\delta_f=60^\circ$. (See fig. 20.)

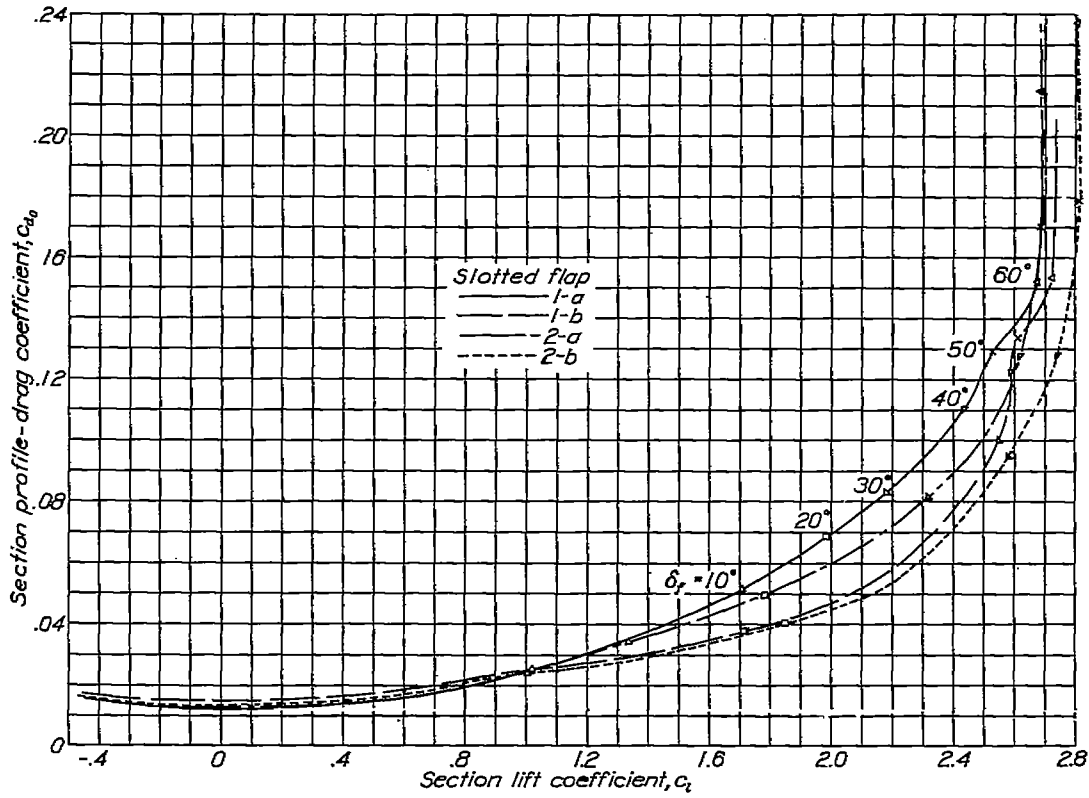


FIGURE 20.—Comparison of profile-drag coefficients for slotted flaps 1-a, 1-b, 2-a, and 2-b.

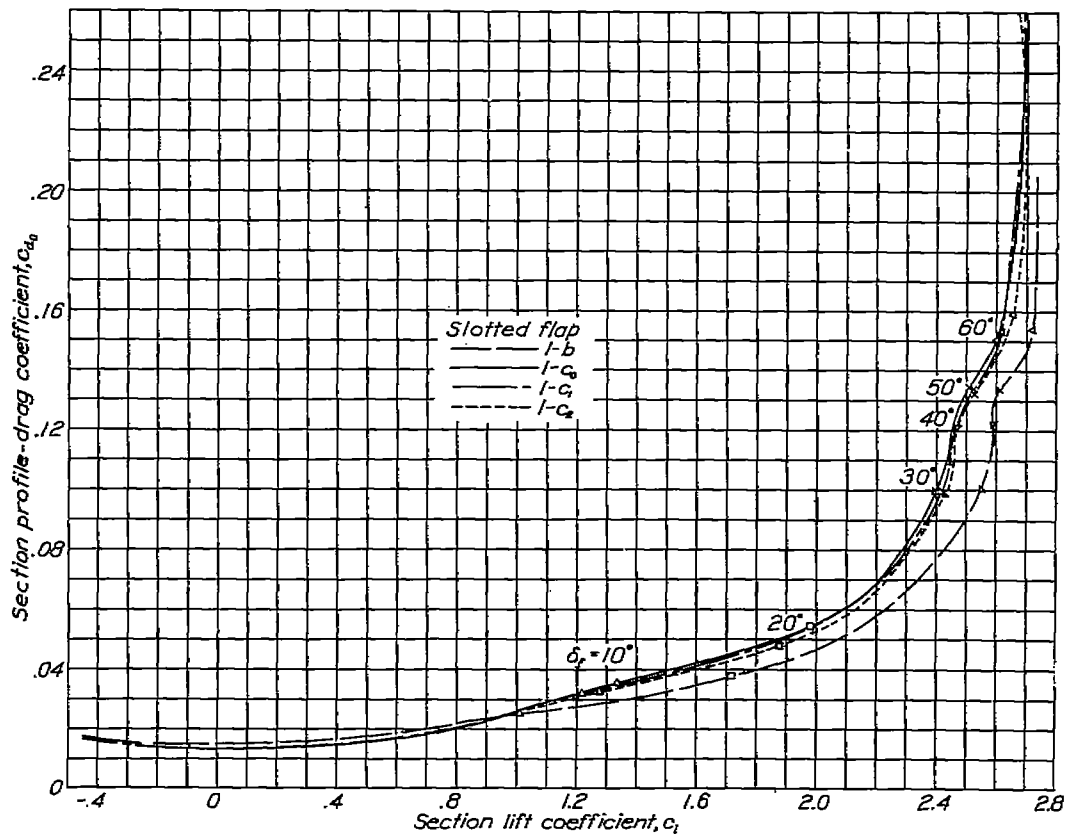


FIGURE 21.—Effect of slot-entry radius on profile-drag coefficient of airfoil.

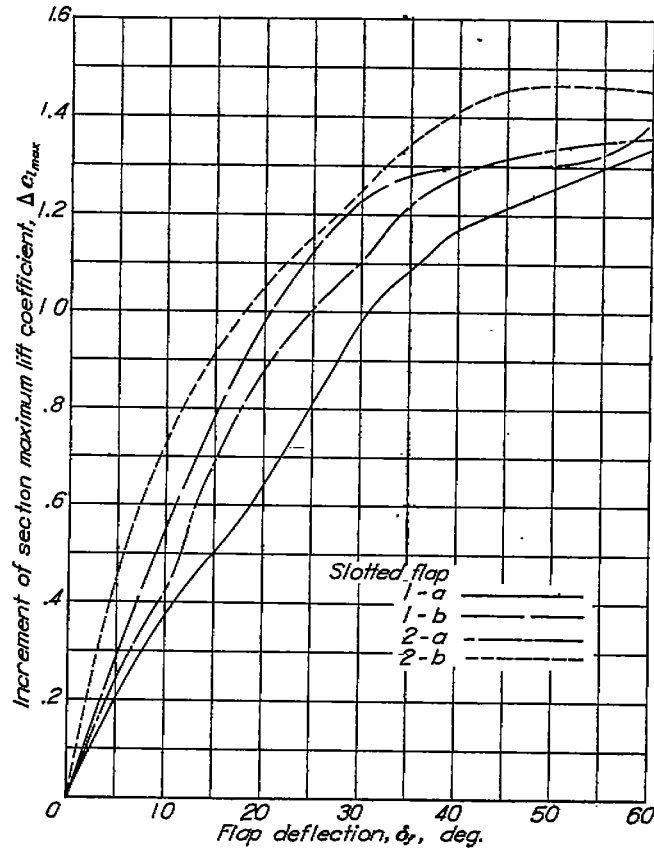


FIGURE 22.—Comparison of increments of maximum lift coefficient for slotted flaps 1-a, 1-b, 2-a, and 2-b when moved and deflected along the selected optimum paths.

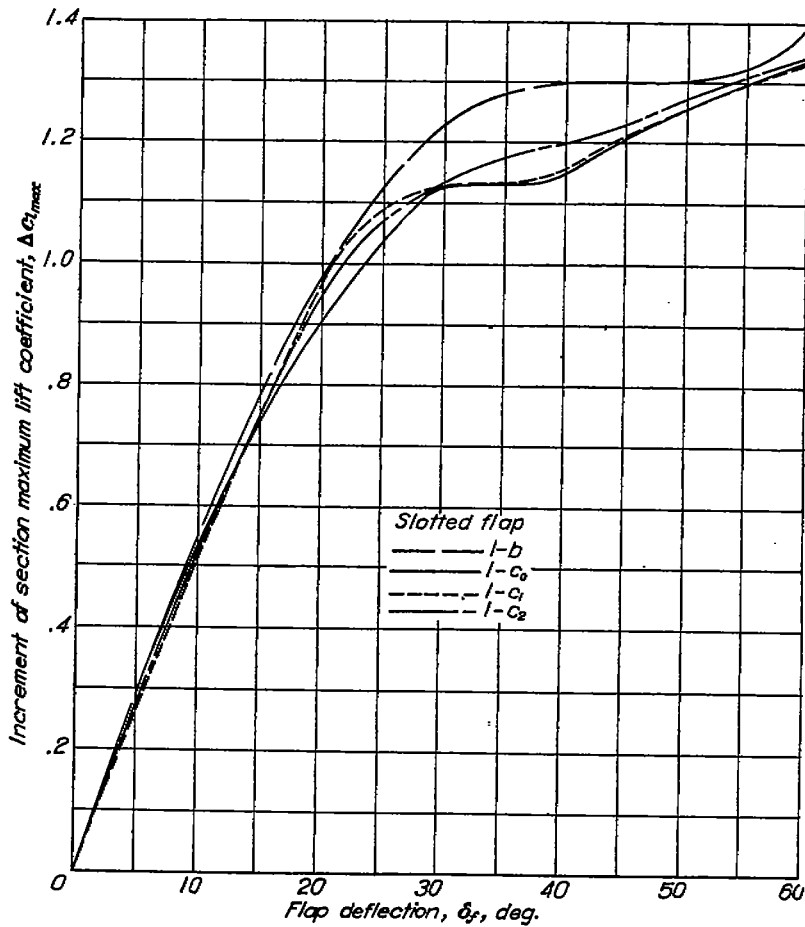


FIGURE 23.—Effect of slot-entry radius on increment of maximum lift coefficient of airfoil when the flaps are moved and deflected along the selected optimum path for flap 1-b.

Reference to figure 16 also shows that, beyond this range of flap deflections, there is practically no change in the pitching-moment coefficient and only about a 1° shift in the angle of attack at a lift coefficient of 2.6 with a 20° change in flap deflection from 60° to 40°.

The tabulated maximum pitching-moment coefficient $c_{m_{max}}$ is the maximum obtained in the useful-flight range. Slotted flaps 2-a and 2-b have the highest, and nearly equal, values of $c_{m_{max}}$, these values being 6 percent higher than any of those for arrangements of flap 1. The pitching-moment coefficients obtained with the slotted flaps on the N. A. C. A. 23021 airfoil are about the same as those obtained for corresponding flap arrangements on the N. A. C. A. 23012 airfoil reported in reference 1.

Comparison with slotted flap on N. A. C. A. 23012 airfoil.—The envelope polars for slotted flap 2-b on the N. A. C. A. 23021 airfoil and for the corresponding slotted flap 2-h on the N. A. C. A. 23012 airfoil (reference 1) are plotted in figure 25 for comparison. The two curves are quite similar, with the curve for the N. A. C. A. 23021 airfoil consistently showing a somewhat higher drag coefficient for all lift coefficients throughout the normal-flight range. The maximum lift for either arrangement is the same. The final selection of airfoil thickness will probably be a compromise between aerodynamic and structural requirements.

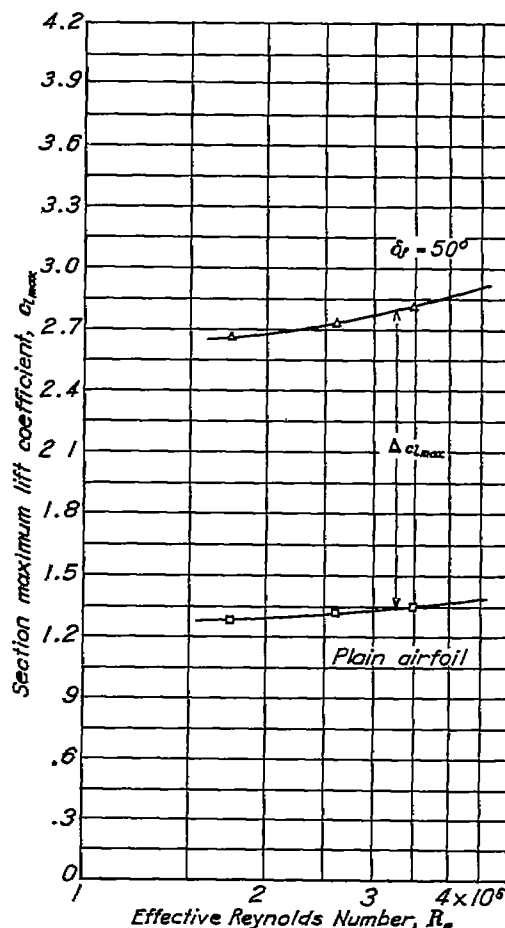


FIGURE 24.—Scale effect on maximum lift coefficient of N. A. C. A. 23021 airfoil with slotted flap 2-b at optimum location.

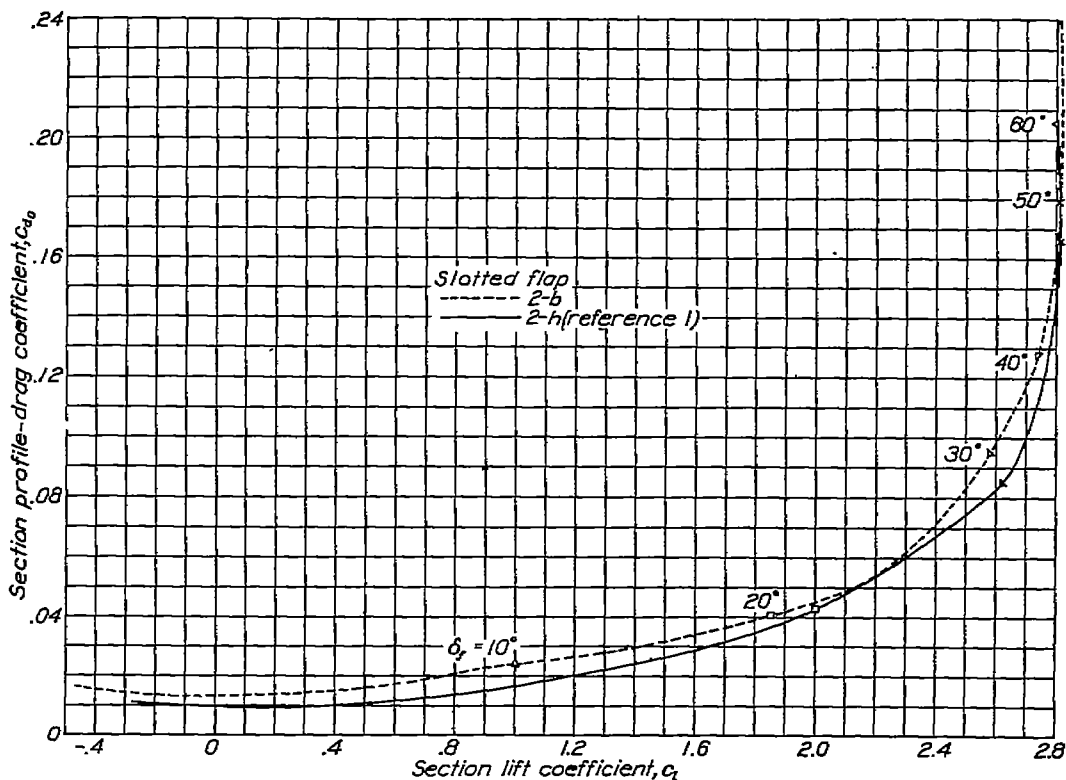


FIGURE 25.—Comparison of slotted flaps on N. A. C. A. 23012 and N. A. C. A. 23021 airfoils.

CONCLUDING REMARKS

If a door were used to close the break in the lower surface of the wing with the flaps neutral, slotted flap 2-b would be superior to any of the flaps tested on the basis of maximum lift coefficient, speed-range ratio, control of the angle of glide, and low drag for take-off and initial climb. Of the other combinations without a door, slotted flap 1-a gave the highest speed-range ratio, but slotted flap 2-b is still superior in other respects. The pitching-moment coefficients were about the same for the slotted flap on the N. A. C. A. 23021 airfoil as for the corresponding arrangements on the N. A. C. A. 23012 airfoil. The final selection of the optimum slotted flap will probably be a compromise in which structural considerations will be the deciding factor.

LANGLEY MEMORIAL AERONAUTICAL LABORATORY,
NATIONAL ADVISORY COMMITTEE FOR AERONAUTICS,
LANGLEY FIELD, VA., February 24, 1939.

REFERENCES

1. Wenzinger, Carl J., and Harris, Thomas A.: Wind-Tunnel Investigation of an N. A. C. A. 23012 Airfoil with Various Arrangements of Slotted Flaps. T. R. No. 664, N. A. C. A., 1939.
2. Wenzinger, Carl J., and Gauvain, William E.: Wind-Tunnel Investigation of an N. A. C. A. 23012 Airfoil with a Slotted Flap and Three Types of Auxiliary Flap. T. R. No. 679, N. A. C. A., 1939.

3. Wenzinger, Carl J., and Harris, Thomas A.: Preliminary Wind-Tunnel Investigation of an N. A. C. A. 23012 Airfoil with Various Arrangements of Venetian-Blind Flaps. T. R. (to be published), N. A. C. A., 1940.
4. Harris, Thomas A.: The 7 by 10 Foot Wind Tunnel of the National Advisory Committee for Aeronautics. T. R. No. 412, N. A. C. A., 1931.
5. Jacobs, Eastman N., and Sherman, Albert: Airfoil Section Characteristics as Affected by Variations of the Reynolds Number. T. R. No. 586, N. A. C. A., 1940.

TABLE I
ORDINATES FOR AIRFOIL AND FLAP SHAPES

[Stations and ordinates in percent of wing chord]

N. A. C. A. 23021 airfoil			Flap 1			Flap 2		
Station	Upper surface	Lower surface	Station	Upper surface	Lower surface	Station	Upper surface	Lower surface
0		0	0		-3.30	0	-0.55	-0.55
1.25	4.87	-2.08	.82	-1.68	-4.63	.32	.59	-1.81
2.5	6.14	-3.14	.64	-.88	-4.82	.64	1.08	-2.30
5	7.93	-4.82	1.28	.84	-4.87	1.28	1.89	-2.88
7.5	9.13	-5.55	1.88	1.28	-4.76	1.93	2.44	-3.29
10	10.08	-6.32	2.67	1.95	-4.64	2.67	2.88	-3.63
15	11.19	-7.51	5.14	3.60	-4.23	5.14	3.96	-3.91
20	11.80	-8.30	7.70	4.28	-3.79	7.70	4.26	-3.79
25	12.05	-8.78	10.27	5.99	-3.34	10.27	3.99	-3.34
30	12.06	-8.95	12.83	3.42	-2.84	12.83	3.42	-2.84
40	11.49	-8.88	15.40	2.83	-2.36	15.40	2.83	-2.36
50	10.40	-8.14	17.96	2.21	-1.86	17.96	2.21	-1.86
60	8.90	-7.07	20.53	1.56	-1.35	20.53	1.56	-1.35
70	7.09	-5.72	23.10	.90	-.81	23.10	.90	-.81
80	5.05	-4.13	25.68	.22	-.22	25.68	.22	-.22
90	2.78	-2.30						
95	1.53	-1.30						
100	.22	-.22						
			Center of L. E. arc			Center of L. E. arc		
L. E. radius: 4.85. Slope of radius through end of chord: 0.305			1.00	-3.90		2.89	-0.55	
			L. E. radius: 1.00			L. E. radius: 2.89		